

Observing Manual

Spartan IR Camera for the SOAR Telescope

Edwin D. Loh

Department of Physics & Astronomy
Michigan State University, East Lansing, MI 48824

Loh@msu.edu 517 884-5612

- 26 October 2006
- 11 July 2007 Revised
- 4 December 2007 Revised
- 15 October 2008 Revised url of remote panels
- 20 December 2008 Added text commands for focusing and offsetting telescope
- 12 August 2009 Added filters & text commands OffsetTo and PrintTCS
- 5 September 2009 Fixed errors in sky map & added Observing Assistant
- 12 November 2009 Added world coordinate system
- 21 February 2010 Updated info on SpartanGUI; clarify use of distortion-induced flat-field
- 15 June 2010 Added "How to focus"

Abstract

This manual, intended for astronomers, contains a description of the instrument, step-by-step instructions on how to perform common observing tasks, and a discussion of the instrument parameters relevant for observing. The graphical user interface SpartanGUI provides the most detailed control of the instrument. In addition, a text-based user interface SpartanTUI allows scripting for more complex or repetitive sequences of operations. To learn to operate the instrument, you may operate the simulated hardware remotely with a web browser.

Contents

1 Instrument description	3
1.1 Optics	3
1.2 Mechanical	7
1.3 Vacuum & Cooling	8
2 Instrument parameters	9
2.1 Wide-field and high-res configurations	9

2.2	Lyot Stop	10
2.3	Filters	12
2.4	Tip-tilt point-spread function	13
2.5	Detector parameters	16
2.6	Orientation of quadrants	17
3	Mapping between the detectors and sky	18
3.1	Flat field	25
3.2	WCS	28
4	Software	30
4.1	SpartanGUI	30
4.2	SpartanTUI	32
4.3	Operating Other Components	34
5	How to	44
5.1	Get a Picture	44
5.2	See Images	44
5.3	Change the Filter	45
5.4	Choose the Pupil Stop	45
5.5	Change Angular Resolution	45
5.6	Change Filename Prefix	46
5.7	Change Object Name	46
5.8	Focus	46
5.9	Focusing assistant	47
6	Text-based Interface	55
6.1	Native Commands	55
6.1.1	Filters	55
6.1.2	Offsetting the telescope using the command offset	56
6.1.3	Offsetting the telescope using the command offsetTo	56
6.2	Scripts	56
6.3	Testing Scripts	57
7	Simulated Camera	60
8	Operation with a Web Browser	60
8.1	Preparation	61
9	Other Documentation	61

1 Instrument description

The Spartan Infrared Camera (Figure 3), operates in the 1–2.4 μ spectral band for imaging with tip-tilt correction of atmospheric turbulence, which the SOAR Telescope provides. It has two focal ratios, wide-field (WF) with 68 mas/pixel for a wide field and high-res (HR) with 41 mas/pixel for high angular resolution. In the high-res configuration, the detectors resolve the diffraction limit in the atmospheric window at $\lambda 1.6 \mu\text{m}$. The detectors are HAWAII-2 arrays, (HgCdTe **Astronomical Wide Area Infrared Imagers** with 2048x2048 pixels). The instrument is cooled with liquid nitrogen.

1.1 Optics

The optics (Figure 1) images the curved focal surface of the telescope onto the detector.

A collimating mirror collimates the light and images the primary onto a stop. A focusing mirror focuses the light onto the detector. A plano-convex lens near each detector flattens the field. The mirrors are off-axis to avoid blocking the beam. There are two focal ratios. To switch between the two focal ratios, rotation stages move the high-res collimator and the wide-field focusing mirror move in or out of the beam. Two fold mirrors make the system more compact.

Two filter wheels allow a large number of filters. The little filter wheel is at the Lyot stop. For the K band, where the stop must be accurate to block thermal radiation, the stop must be in the little wheel and filters must be in the big wheel.

A mask wheel at the telescope focus holds the field stops and masks for coronagraphy or slits for spectroscopy.

Let us follow the path of a light ray in the optical schematic (Figure 1). The principal ray for the wide-field channel is red; it is blue for the high-resolution channel.

Window The flat, CaF₂ window separates the cold vacuum inside and the warm outside.

Because the window radiates into about 0.9 steradian of cold, it may cool below the dew point on very humid days. Some nitrogen boil-off, after being warmed in a length of pipe, blows on the window to purge the surrounding air of water.

Thermal reflector Thermal infrared radiation ($\lambda 10 \mu$), emitted by the window into the instrument over a 2π solid angle, is a large heat load. The thermal reflector¹, a

¹Loh, E., 2004a, Thermal reflector to reduce thermal radiation in the entrance of cryogenic instruments, SPIE 5492, 1661, <http://www.pa.msu.edu/~loh/SpartanIRCamera/SPIE%205492-115.pdf>

hemispherical mirror and a flat mirror, reduces the heat load by a factor of 3. Of course there is an opening into the rest of the instrument for the wanted light. The thermal radiation that does not enter the opening reflects back to the window.

Mask wheel The telescope focal surface is at the mask wheel. Masks for blocking the light of bright stars may be inserted by rotating the wheel. The focal surface of the telescope is a sphere of radius 960 mm centered outside the instrument. At the edge of the field, the focus is 3.27 mm closer to the primary mirror. The astigmatism of the telescope means there is a 0.65 mm difference between the sagittal and tangential focus at 4 arcmin from the center of the field. There is a small amount of coma.²

Dewar for liquid nitrogen The light path is through a cut-out in the dewar.

Collimating mirrors image the primary mirror of the telescope onto the pupil stops. The mirror for the wide-field channel is fixed on a post. A mechanism inserts the collimating mirror for the high-resolution channel into the beam.

Fold mirror #1 Without the two fold mirrors, the instrument object and image would be coincident, and the size of the instrument would be doubled. The folds are $\phi 90$ -mm flat mirrors.

Big filter wheel has 19 positions. The filters are $\phi 50$ mm. For more detailed requirements for filters, see Loh 2004³

Little filter wheel is used primarily for Lyot stops. The collimating mirror images the telescope primary mirror on a surface at the little filter wheel. There are four stops: tight and loose for the high-res and wide-field channels. The tight stops are conservative: they block light that originates off of the primary mirror for *any* field positions. For some field positions, useful light is blocked. The shadow of the secondary mirror is blocked also. The loose stops are liberal: they block light that originates off of the primary mirror for *every* field position. The spiders that hold the secondary mirror are not blocked in either case. See Figure 5 and §2.2.

Fold mirror #2

²Loh, E., 2002, Interface requirements, Spartan IR Camera, <http://www.pa.msu.edu/~loh/SpartanIRCamera/RequirementInterface3.PDF>

³Loh, E., 2004, Requirements for Filters, Spartan IR Camera for the SOAR Telescope, <http://www.pa.msu.edu/~loh/SpartanIRCamera/RequirementInterface3.PDF>

Camera mirror together with the collimating mirror reimages the f/16 beam to f/22 or f/13.

Pyramidal mirror separates the field into four sections in order to allow the detectors, which occupy a large space beyond the sensing area, to cover fields that are close together in the sky.

Field-flattening lens corrects the field curvature of the telescope and the instrument. The plano-convex, CaF₂ lens moves the image at the center of the field back with respect to that at the edge of the field.

Four detectors are on the 4-eye assembly, which independently tilts each detector by 9° when switching between the HR and WF channels.

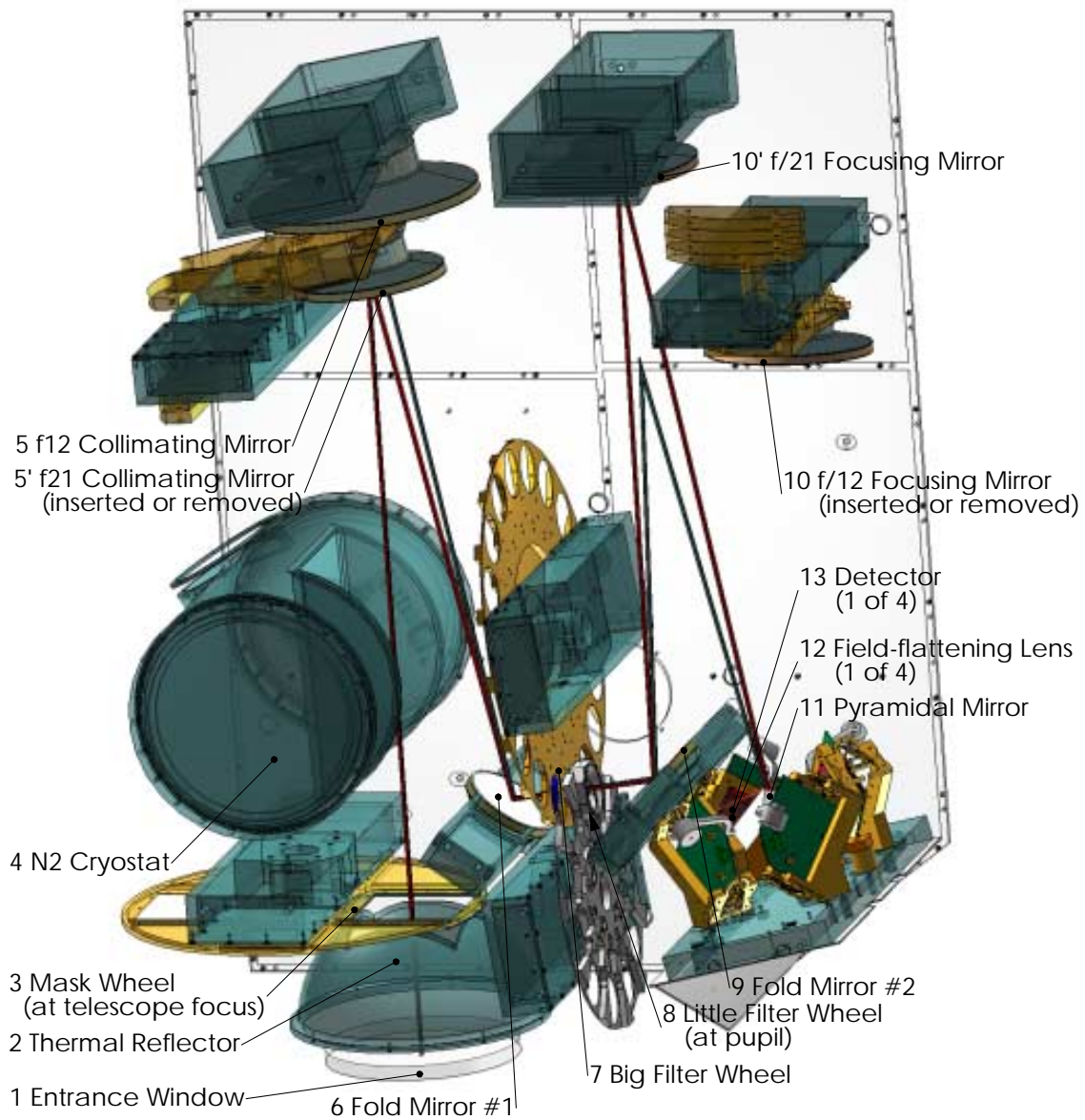


Figure 1: Schematic of the instrument oriented with the front of the instrument down and the top toward the viewer. The mirrors and 4-eye are positioned for the high-resolution mode. The principal ray is the blue line for the wide-field mode and red for high-resolution.

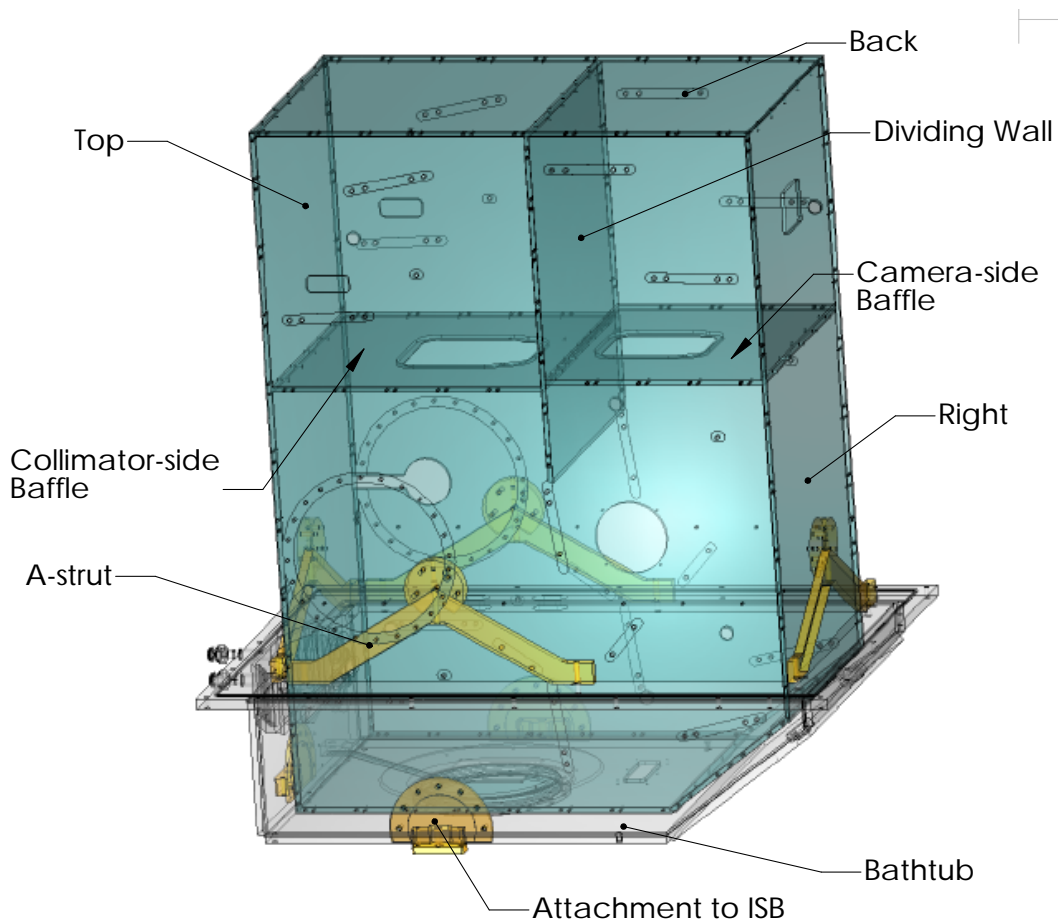


Figure 2: Cryo-optical box inside the bathtub of the vacuum enclosure

1.2 Mechanical

The optics and cryostat for nitrogen (Figure 1) mount on the top and bottom of the cryo-optical box (COB) (Figure 2). As the Nasmyth rotator turns to compensate for the rotation of the field, the instrument turns along an axis perpendicular to the large plates of the COB, which is approximately perpendicular to the paper in Figure 1.

The COB mounts on the bathtub (Figure 2) of the vacuum enclosure through four A-struts. The legs of the A-struts are G-10 fiberglass, a stiff, insulating material. The vacuum lid mates to the bathtub at a flange to complete the vacuum enclosure.

The instrument attaches to the instrument selection box (ISB) on the telescope through three Flamant transitions, semicircular plates that allow movement to compensate for the difference in thermal expansion of the aluminum instrument and steel ISB.

1.3 Vacuum & Cooling

The vacuum enclosure consists of a bathtub and lid, which mate at a flange visible in Figures 3 & 2.

Liquid nitrogen cools the instrument. The cryostat holds 7 L of nitrogen independent of rotation along an axis perpendicular to the top, which is the rotation axis of the instrument on the telescope.

A cryogenic charcoal getter pumps oxygen, nitrogen, and argon, which permeate through the Viton o-rings.

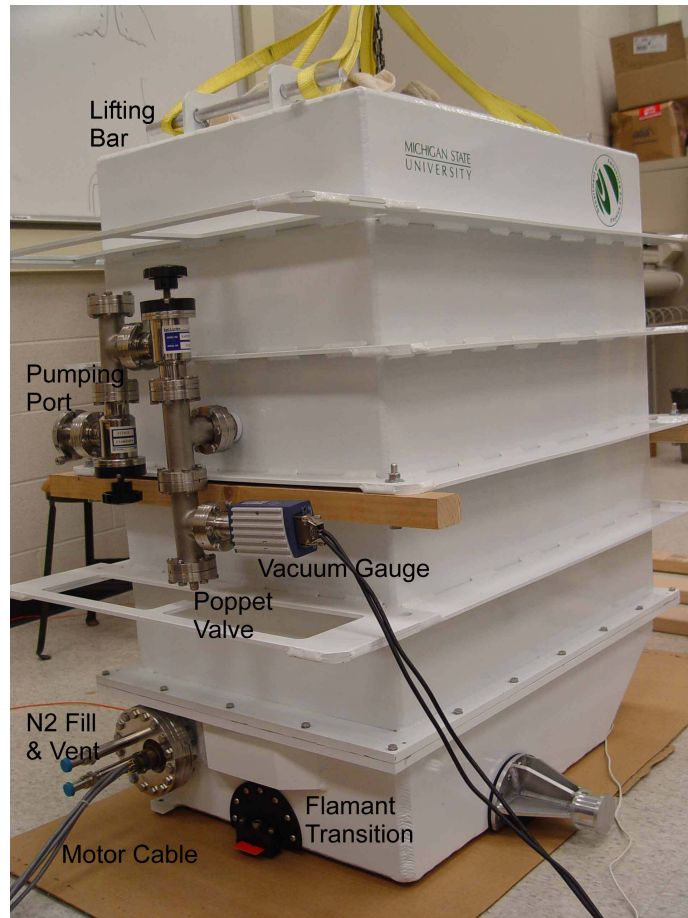


Figure 3: Spartan Camera

2 Instrument parameters

2.1 Wide-field and high-res configurations

Configuration	Pixel size [mas]	Field size		Blank strip [arcmin]	Offset [arcmin]
		Edge-edge [arcmin ²]	Single detector [arcmin ²] [pixel]		
Wide-field	68.47	5.17 × 5.12	2.34 × 2.32 2048 ²	0.47	(−1.31, −1.41) (1.51, −1.40) (1.51, 1.40) (−1.31, 1.41)
High-resolution	41.38	3.08 × 3.14	1.42 × 1.40 2048 ²	0.28	(−0.78, −0.85) (0.90, −0.86) (0.90, 0.86) (−0.78, 0.85)

Table 1: Parameters of the wide-field and high-resolution configurations. The offsets are from the field center to the center of each of the four detectors.

The Spartan Camera has two plate scales, wide field (WF) at 68 mas/pixel and high resolution (HR) at 41 mas/pixel. (See Table 1.) With the HR channel, the detectors resolve the diffraction limit in the atmospheric window at $\lambda 1.6 \mu\text{m}$. With the WF channel, the field coverage is large, and the tip-tilt correction is fairly uniform across the field.

The four detectors map into the sky approximately as a 3.1×3.1 arcmin square with blank 0.3 arcmin-wide strips for the HR channel and as a 5.1×5.2 arcmin square with blank 0.5 arcmin-wide strips for the WF channel. See Figure 4.

Figure 4 is drawn as the images would appear on a display screen: the origin is at the lower left corner of each detector, and rows are horizontal. The actual orientation in the sky depends on the instrument rotator.

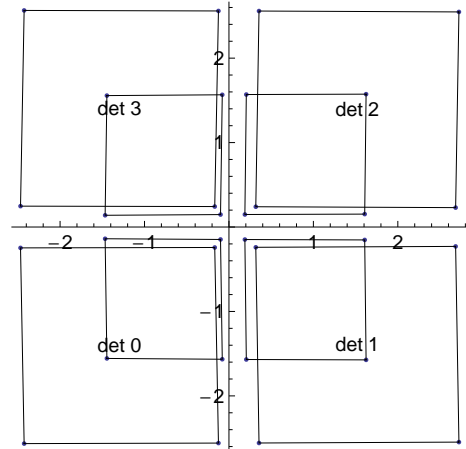


Figure 4: Map of the four detectors, numbered 0–3 in the sky for the HR (smaller field) and WF (larger field) channels. The scale is arcmin.

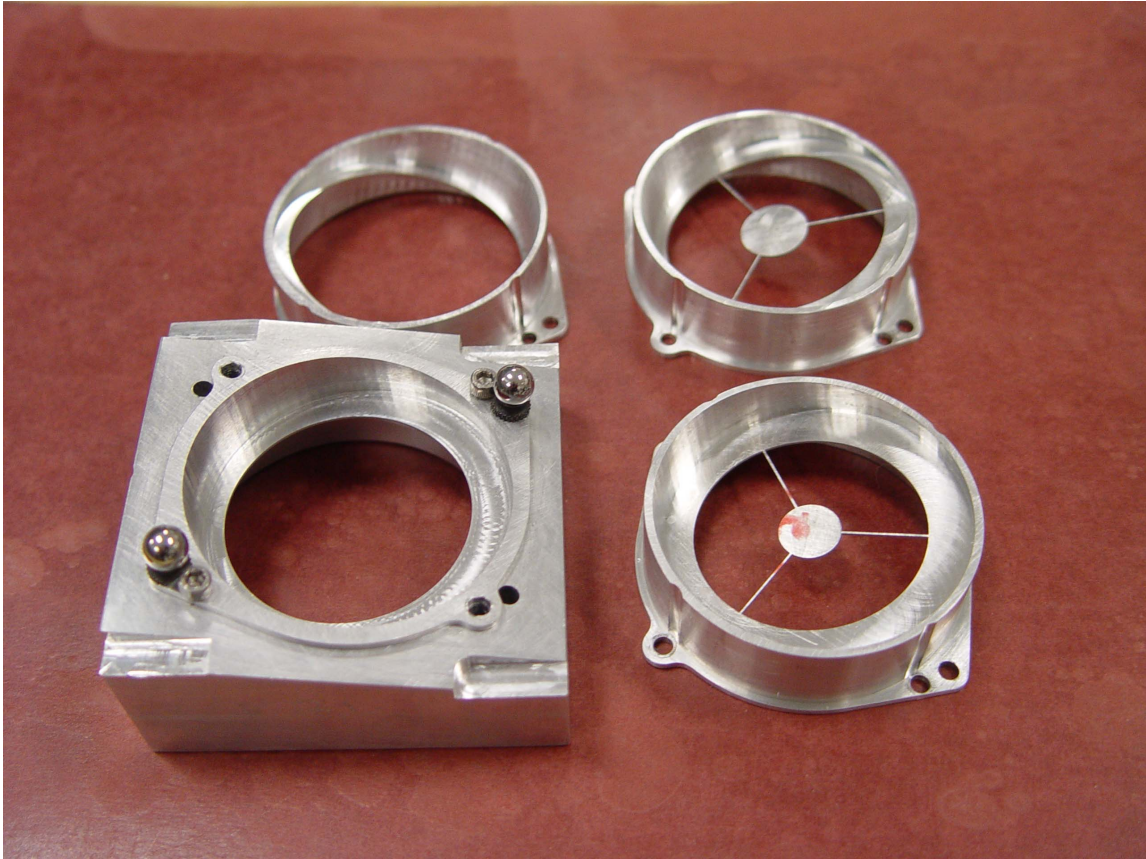


Figure 5: LR-loose (in the machining jig), LR-tight, WF-tight, and WF-loose Lyot stops (in counter-clockwise order)

2.2 Lyot Stop

The Lyot stop, placed at the image of the primary mirror, blocks light that comes from the telescope structure and other parts of the observatory. For each focal ratio, there are two stops (Figure 5). The tight stop blocks all light that originates off of the primary mirror. For some field points, it blocks light that comes from the primary mirror. It blocks the secondary mirror but not the spiders that hold the secondary mirror. The loose stop blocks light that originates off of the primary mirror for all field positions; *i. e.*, for some field positions, the stop allows light from off of the primary. The loose stop does not block the secondary mirror.

The tight stop must be used for the K band, where the short-wavelength tail of thermal radiation is significant. If the loose Lyot stop is used, thermal radiation from the edges of

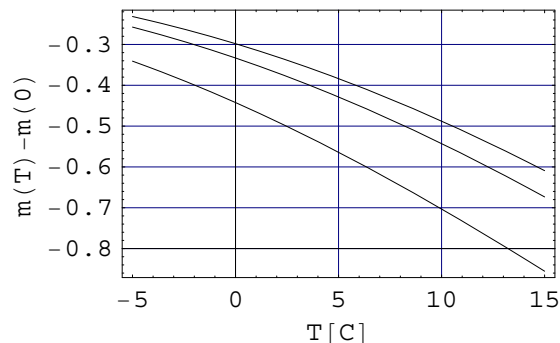


Figure 6: Limiting magnitude vs temperature in the K band compared with that of a perfectly reflecting telescope. In order from top to bottom, the cases are (1) spider and central hole blocked, (2) central hole blocked (the case with tight Lyot stops), and (3) spider and central hole unblocked (the case with loose Lyot stops). In the model, temperature affects thermal emission of the telescope only and not that of the sky.

the primary and the hole in the primary are not blocked. For the K band, thermal emission of the hole in the primary mirror makes the limiting magnitude brighter by 0.16 mag for a temperature of 10 C (Figure 6).⁴

The thermal radiation of the edge of the primary is yet to be determined, since masking the defects on the edge of the mirror has not been decided. The image of the pupil stop on the primary mirror shifts slightly with field position. The image is centered on the primary mirror for field positions halfway from the center of the field. For the center of the field and the periphery, the image is not concentric with the primary mirror, and the thermal emission will be worse with the loose Lyot stops.

Thermal emission in the J and H bands is negligible.

⁴ The estimated emissivity of the four warm mirrors (primary, secondary, tertiary, and dichroic) is 7%. The effective emissivity of the hole of the secondary is 6%. (The hole is assumed to be black and it covers 6% of the primary; we have not figured out the actual path of that light.) The effective emissivity of the spider is 1.6%. The model uses the sky brightness of Simons and Tokunaga 2002.

2.3 Filters

The filters are the Mauna Kea (MK) J, H, and K filters (Table 2), a Y-band filter, and spectral line filters (Table 4). The MK filters⁵ were defined to optimize photometric accuracy by avoiding wavelengths where atmospheric absorption is heavy.

The parameters for the MK filter and estimated sky backgrounds are in Table 2. The sky background is based on Simons & Tokunaga 2002 with these modifications: There are four warm mirrors each with an emissivity of 1.9%, and the ambient temperature is 10 C.

Exposure times to match detector noise and saturation magnitudes are in Table 3.

Sometimes there is need for observing bright stars, and many of the standard stars of Hawarden et al. 2001⁶ and Persson et al. 1998⁷ are too bright to use. Two solutions are possible. Shutting off tip-tilt correction reduces the intensity in the center of the star by 0.9–1.5 mag. A neutral density filter, ND1, is available with a reduction of 2.25 and 2.5 mag for the HR and WF channels.

The saturation magnitudes were calculated with the tip-tilt corrected point-spread functions for median seeing conditions (Figure 8). With the neutral density filter, the saturation magnitude is brighter than that due to the reduction in the total amount of light. In addition, diffraction reduces the peak intensity.

Since the neutral density filter is actually a plate placed at the pupil with an off-center

Filter	λ (μm)	$d\lambda$ (μm)	τ	B_{HR}	B_{WF}
J	1.25	0.16	0.77	17	67
H	1.64	0.29	0.79	200	800
K	2.20	0.34	0.75	42	170

Table 2: Parameters for the MK filters (Simons & Tokunaga 2002). The wavelengths for which the filter transmission is 50% at $\lambda \pm \frac{1}{2}d\lambda$. The transmission of the atmosphere is τ . B_{HR} and B_{WF} are the sky background.

Filter	t_{BL} (s)	t_{BS} (hr)	m_{Sat}		
			TT	no TT	ND1
J–HR	100	20	10.4	9.5	7.1
H–HR	8	1.4	10.9	9.7	7.2
K–HR	30	4	11.7	10.2	7.7
J–WF	40	6	11.5	10.6	7.7
H–WF	3	0.5	12.0	10.8	7.8
K–WF	9	1.5	12.8	11.3	8.2

Table 3: Exposure time t_{BL} for the noise of the background to match the detector noise, t_{BS} for the sky to saturate the detector, and the magnitude m_{Sat} of a star that saturates in a 9-s exposure with tip-tilt correction, with natural seeing, and with neutral density filter ND1 and natural seeing.

⁵D. A. Simons, D., & Tokunaga, A., 2002, “The Mauna Kea Observatories Near-Infrared Filter Set. I. Defining Optimal 1–5 Micron Bandpasses,” PASP 114, 169.

⁶Hawarden, T. G., et al., 2001, “JHK standard stars for large telescopes: the UKIRT Fundamental and Extended lists,” MNRAS 325, 563. The stars are between 9.4 and 15.0 mag.

⁷Persson, S. E., et al., 1998, AJ, 116, 2475. The stars are between 10.5 and 12.5 mag.

hole, several complications arise. For the high-res channel, ND1 reduces the light by an additional 0.25 mag, since the pupil is smaller. The image of a star is wider than that taken without the neutral density filter. (Compare the bottom right panel of Figure 8 with the other panels.) Finally, at certain angles of the Naysmyth instrument rotator, the spider of the secondary mirror shadows the hole. When this occurs, the transmission drops by 0.024 and 0.027 mag for the WF and HR channels.

Filter	λ (nm)	$d \lambda$
Y	1020	200
HeI	1083	10
[FeII]	1644	15
Cont. 1	2045	30
HeI/CIV	2070	30
H2	2121	20
Cont. 2	2140	30
Br γ	2161	20
Cont. 3	2210	30
CO	2325	70

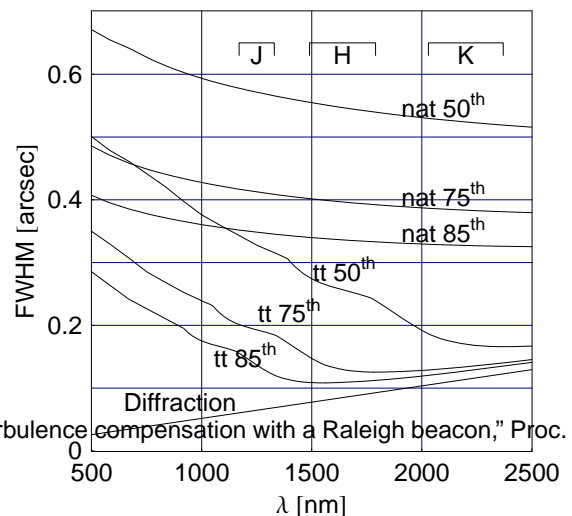
Table 4: Y-band and narrow-band filters

2.4 Point-spread function with tip-tilt correction for atmospheric turbulence

Point-spread functions (PSF) were computed for natural seeing and for tip-tilt correction for atmospheric turbulence. Fried's parameter r_0 is assumed to be 15 cm at λ 500 nm (Seeing is 0.68 arcsec.) for median seeing conditions and 20 and 25 cm for 75-th and 85-th percentile conditions.⁸

With tip-tilt correction, the point-spread function is not a gaussian. At longer wavelength and better seeing, the PSF is approximately the sum of a diffraction spike,

⁸Tokovinin, et al., 2004, "Design of ground-layer turbulence compensation with a Raleigh beacon," Proc. SPIE, 5490, 870-878.



13

Figure 7: Width of a star v.s. wavelength for natural seeing and for tip-tilt correction. Seeing conditions are 50-th, 75-th, and 85-th percentiles, for which $r_0 = 15, 21,$ and 25 cm, respectively, at λ 500 nm. The atmospheric bands J, H, and K are marked.

which has the width of the Airy function, and a smoother part. At shorter wavelengths, the shape is more complex. (See Figure 8 for the PSF and Figure 7 for the width of the PSF.)

For median seeing in the K band and the top quartile in the H band, images are expected to resolve the diffraction limit, since there is a significant amount of light in the diffraction spike.

The intensity at angle $r = \theta D / \lambda$ is

$$I(r) = 2\pi \int_0^1 J_0(2\pi r x) M(x) x dx,$$

where the modulation transfer function

$$M_{\text{nat}}(x) = M_{\text{diff}}(x) e^{-3.44 \left(\frac{Dx}{r_0}\right)^{5/3}}$$

for natural seeing,

$$M_{\text{tt}}(x) = M_{\text{diff}}(x) e^{-3.44(1-x^{1/3}) \left(\frac{Dx}{r_0}\right)^{5/3}}$$

for seeing with tip-tilt correction for atmospheric turbulence, and

$$M_{\text{diff}}(x) = \frac{2}{\pi} \left[\arccos x - x(1-x^2)^{1/2} \right]$$

with no atmosphere.⁹ The telescope diameter is D . x is the spatial frequency scaled by $(f\lambda)^{-1}$, where f is the focal ratio and λ is the wavelength.

If the sky is the dominant noise, then the variance of the light A in a star with optimal estimation is $\sigma^2 \left(\int I(r)^2 \right)^{-1}$, where σ is the noise in the sky. $A = \int hI / \left(\int I^2 \right)$, where h is the image of the star.

With natural seeing, the magnitude of the faintest detectable star depends on image width w as $-2.5 \log w$, but with tip-tilt correction, the limiting magnitude depends on D/r_0 in a more complicated way, since the form of the point-spread function changes (Figure 8). For natural seeing, the change in limiting magnitude is practically independent of wavelength, but it does depend on wavelength for tip-tilt corrected images (left panel of Figure 9).

⁹Chanan, G., et al., 1994, "Adaptive Optics for Keck Observatory," Keck Observatory Report No. 208.

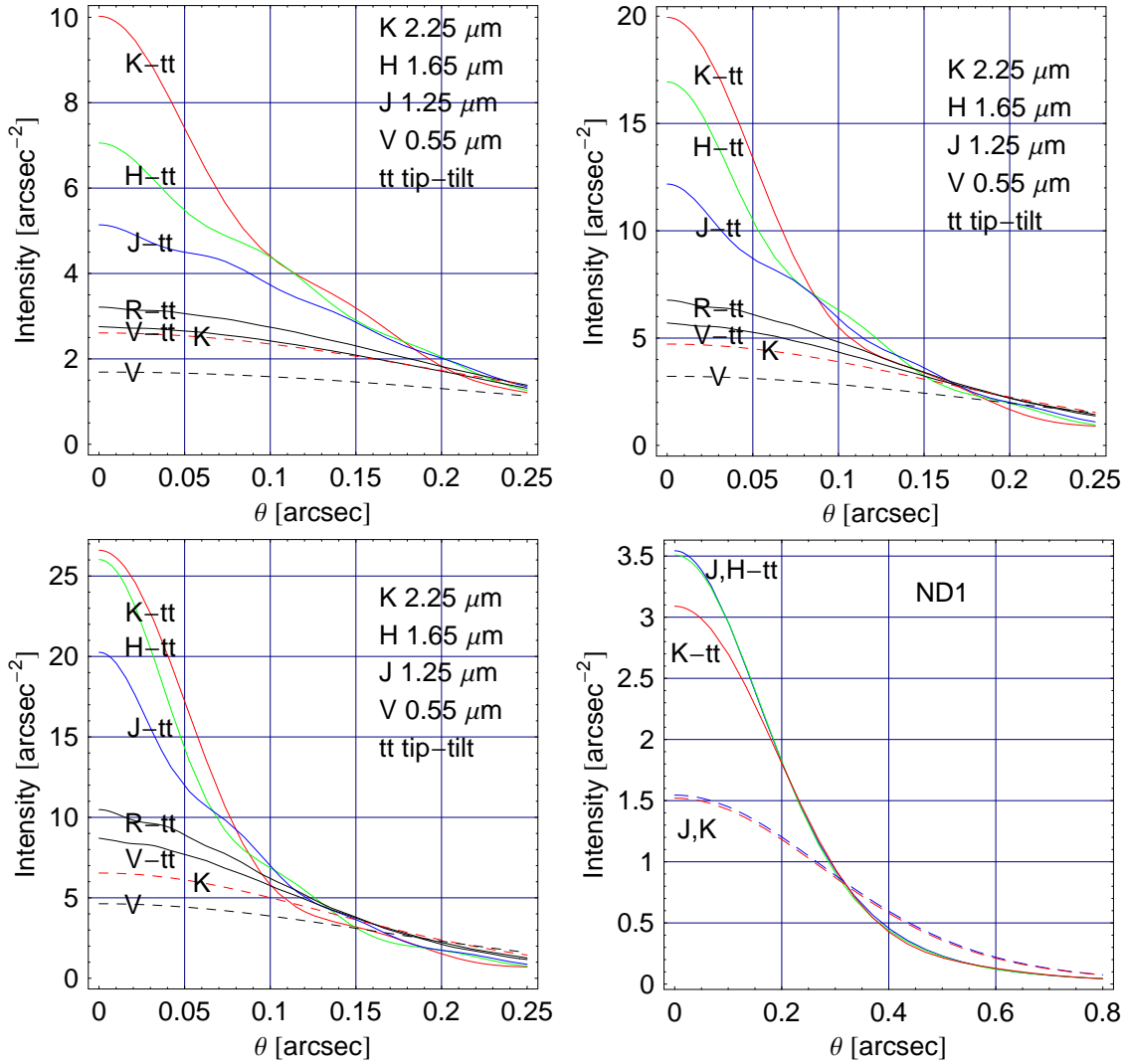


Figure 8: Point-spread functions for natural seeing (dashed line) and with tip/tilt correction for atmospheric turbulence (solid lines) for median (top left), top-quartile (top right), 85-th percentile (bottom left), and median (bottom right with neutral density filter ND1 in the WF channel) seeing conditions. Without the neutral density filter, the half width of the Airy diffraction function occurs at $\theta = 0.07$, 0.05 , and 0.04 arcsec for the K, H, and J bands. The integral of the point-spread function is 1.

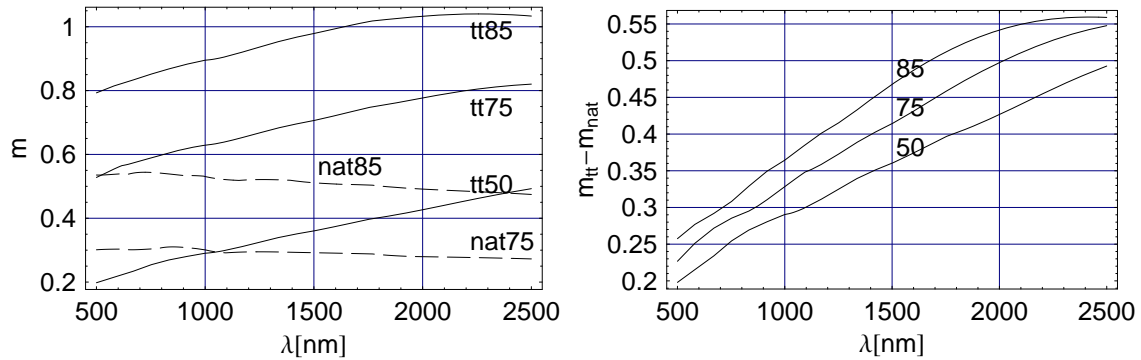


Figure 9: Left: Limiting magnitude vs wavelength for tip-tilt correction (solid line) and for natural seeing (dashed lines) relative to that for natural seeing and median seeing conditions. Right: Improvement in limiting magnitude with tip-tilt correction vs wavelength. The seeing conditions are 50th, 75th, and 85th percentiles.

Besides resolving finer features, tip-tilt correction also reaches fainter magnitudes (right panel of Figure 9). In the K band for example, compared with median natural seeing, the limiting magnitude for natural seeing is fainter by 0.3 and 0.5 mag for the 75th and 85th percentiles of seeing, but with tip tilt correction, the limiting magnitude is fainter by 0.5, 0.8, and 1.1 mag for the 50th, 75th and 85th percentiles. Thus tip-tilt increases the depth by about 0.5 mag in the K band.

2.5 Detector parameters

Detectors	4
Pixels/detector	2048 × 2048
Pixel size	18 × 18 μm
Saturation	≈ 25 kADU
	≈ 75 ke^-
Read noise	≈ 3 ADU
	≈ 10 e^-
Dark current	0.8–3 ADU
	0.3–0.9 e^-

Table 5: Detector parameters. The read noise is that of the difference between a long and a short image.

2.6 Orientation of quadrants

Each detector is split into quadrants, and certain detector artifacts depend on the rows and columns of each quadrant. Even though the rows and columns of each quadrant are rotated, and each detector is rotated, the images are saved on disk so that the directions in the sky of rows (and columns) are the same for all four detectors. See the right panel of Figure 10. The orientation on a display is rotated from that in the sky by a single angle common to all detectors. The left panel of Figure 10 shows the directions for each quadrant.

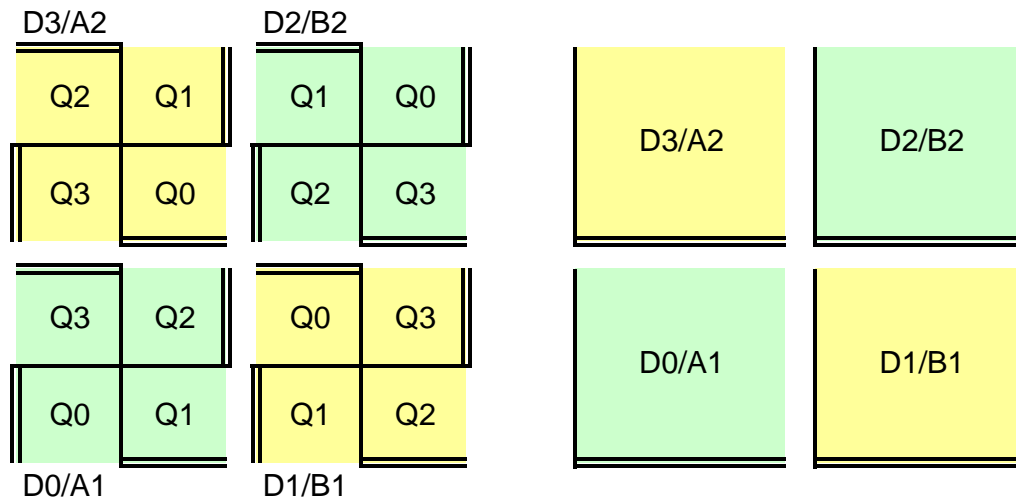


Figure 10: Arrangement of the detectors (labeled D0–D3) and quadrants (labeled Q0–Q3). (The designations A1, A2, B1, and B2 indicate locations in 4-eye.) The left panel shows individual quadrants; the right panel shows the quadrants combined, which is the default way in which the images are written on disk. For each detector or quadrant, the double line is the x-axis, and the single line is the y-axis, where the x-coordinate increases more rapidly in the data stream of the image and usually appears horizontally on a display.

3 Mapping between the detectors and sky

The position on the detector (x, y) maps to an angle (θ_x, θ_y) in the sky. The instrument is mirror-symmetric in the y -direction. We use detector coordinates that run in the x and y -directions from -1 to $+1$ for each detector. The sky coordinates are in pixels of 68.47 and 41.38 mas for the wide-field and high-res channels.

For a linear map without skew,

$$\theta_x(x, y) = a_0 + a_1x \quad (1)$$

$$\theta_y(x, y) = b_0 + b_1y, \quad (2)$$

and the root-mean-square residual is (10, 3) pixel for the wide-field channel (first row of Table 7). A plot of the residuals (top-left panel of Figure 11) shows a rotation of the field. Fitting with skew terms

$$\theta_x(x, y) = a_0 + a_1x + a_2y \quad (3)$$

$$\theta_y(x, y) = b_0 + b_1y + b_2x, \quad (4)$$

reduces the residual.

The detector centers and the linear transformation between the detector and sky are sufficient for many purposes, and these are given in Table 6, where the linear transformation is expressed as $100 \begin{pmatrix} a_1 - 1 & b_2 \\ a_2 & b_1 - 1 \end{pmatrix}$. With these terms, the RMS error is (150, 46) mas for the wide-field channel and (100, 34) mas for the high-res channel. The magnification varies by 2%, and the skew is about 2%, which is 1° .

Det.	Center [arcsec]		Linear transformation	
	WF	HR	WF	HR
0	(-78.69, 84.31)	(-47.04, -51.24)	$\begin{pmatrix} -1.1 & 0.2 \\ -1.9 & -0.3 \end{pmatrix}$	$\begin{pmatrix} -2.7 & -0.6 \\ -1.5 & 0.9 \end{pmatrix}$
1	(90.54, -83.74)	(53.91, -51.76)	$\begin{pmatrix} 1.8 & 0.4 \\ -1.7 & -0.3 \end{pmatrix}$	$\begin{pmatrix} 1.0 & -0.3 \\ -1.2 & 1.1 \end{pmatrix}$
2	(90.54, 83.74)	(53.91, 51.76)	$\begin{pmatrix} 1.8 & -0.4 \\ 1.7 & -0.3 \end{pmatrix}$	$\begin{pmatrix} 1.0 & 0.3 \\ 1.2 & 1.1 \end{pmatrix}$
3	(-78.69, 84.31)	(-47.04, 51.24)	$\begin{pmatrix} -1.1 & -0.2 \\ 1.9 & -0.3 \end{pmatrix}$	$\begin{pmatrix} -2.7 & 0.6 \\ 1.5 & 0.9 \end{pmatrix}$

Table 6: Detector centers and the linear transformation from the detector to sky.

Fitting with quadratic terms

$$\theta_x(x, y) = a_0 + a_1x + a_2y + a_3x^2 + a_4xy + a_5y^2 \quad (5)$$

$$\theta_y(x, y) = b_0 + b_1y + b_2x + b_3x^2 + b_4xy + b_5y^2, \quad (6)$$

reduces the residual, but a barrel distortion remains (top-right panel of Figure 11). The barrel distortion is caused by the field-flattening lenses, each of which is close to its detector.

With barrel distortion removed,

$$\theta_x(x, y) = a_0 + a_1x + a_2y + a_3x^2 + a_4xy + a_5y^2 + a_6x(x^2 + y^2) \quad (7)$$

$$\theta_y(x, y) = b_0 + b_1y + b_2x + b_3x^2 + b_4xy + b_5y^2 + b_6y(x^2 + y^2), \quad (8)$$

and the root-mean-square residual is (0.03, 0.01) pixel for the wide-field channel and (0.02, 0.01) pixel for the high-res channel. See Table 8 for the coefficients a_i and b_i , $i = 0, \dots, 6$. Because of the symmetry of the instrument in the y -direction, detectors 1 and 2 are symmetric, and detectors 0 and 3 are symmetric. The terms that have an odd power of y are relatively odd for a_i and even for b_i when comparing detectors 1 and 2 (or 0 and 3).

Since the detector coordinates in the x and y -directions run from -1 to $+1$, and the sky coordinates are in pixels of 68.47 and 41.38 mas, the center of the field is (a_0, b_0) for each detector, and the maximum contribution of the i -th term can be read readily from (a_i, b_i) . For example, the barrel distortion at the edge of detector 0 is 2(2.5, 2.6) pixel in the wide-field channel.

The field-flattening lens mostly accounts for the terms a_6 and b_6 . Because of this, they are nearly equal, which signifies that the effect has rotational symmetry. In addition, they are nearly equal for the wide-field and high-res channels.

The results in this section are derived from the specification of the telescope¹⁰ and the optical design of the instrument. Fabrication and alignment errors in the instrument and telescope will modify the results. The plate scale and errors in positioning the detector affect all terms in Table 8.

¹⁰Loh, E., 2002, Interface requirements, Spartan IR Camera, <http://www.pa.msu.edu/~loh/SpartanIRCamera/RequirementInterface3.PDF>

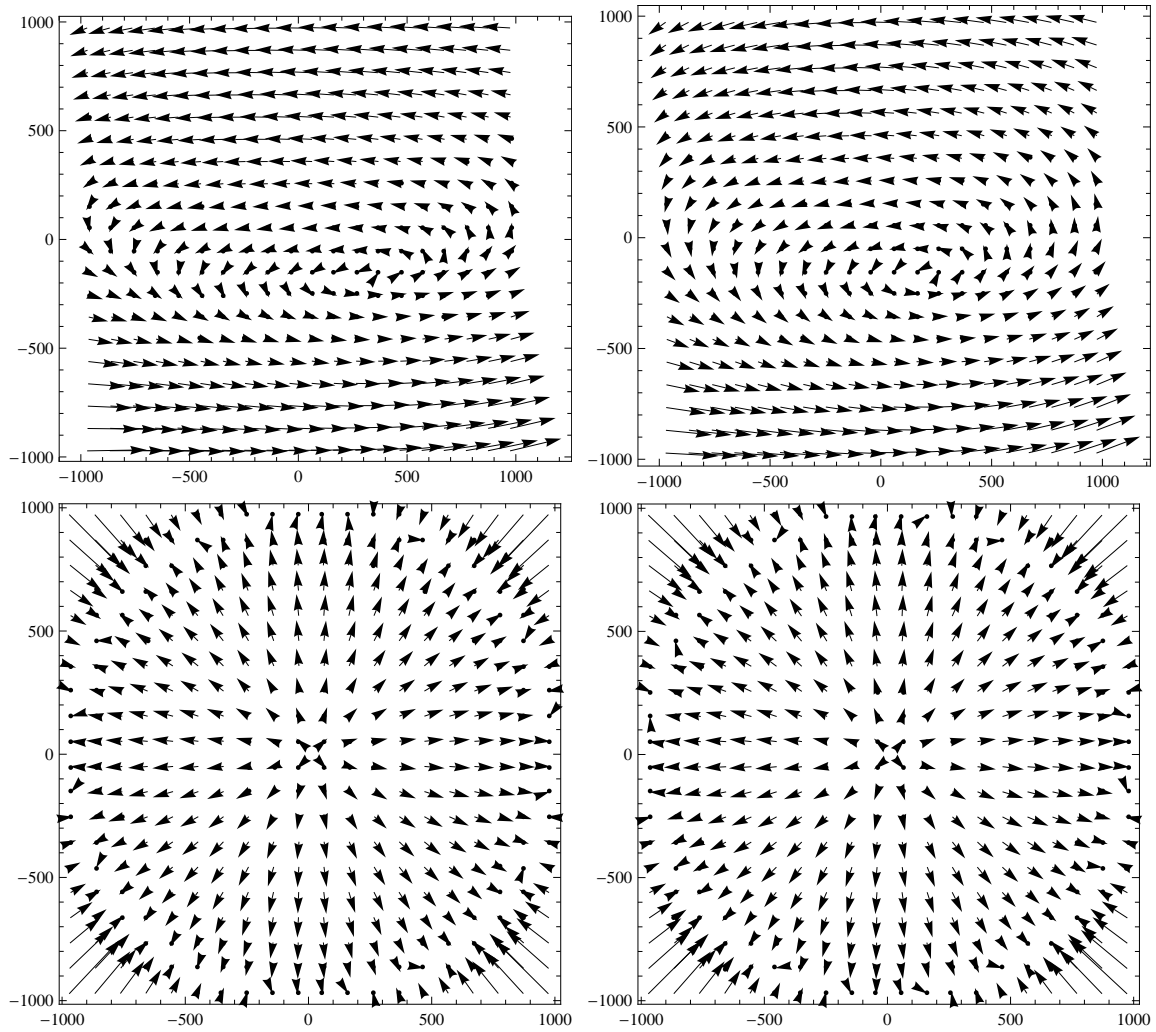


Figure 11: Residuals of the fits in Table 7 for the wide-field channel for detector 0 (left) and 1 (right). Top: linear fit (residuals magnified by 10). Bottom: fit with linear, skew, and quadratic terms (residuals magnified by 100). The scale is pixels. The points are on a 100x100 pixel grid. For the residuals of all four detectors, flip the residuals of detector 0 and 1 along the top edge.

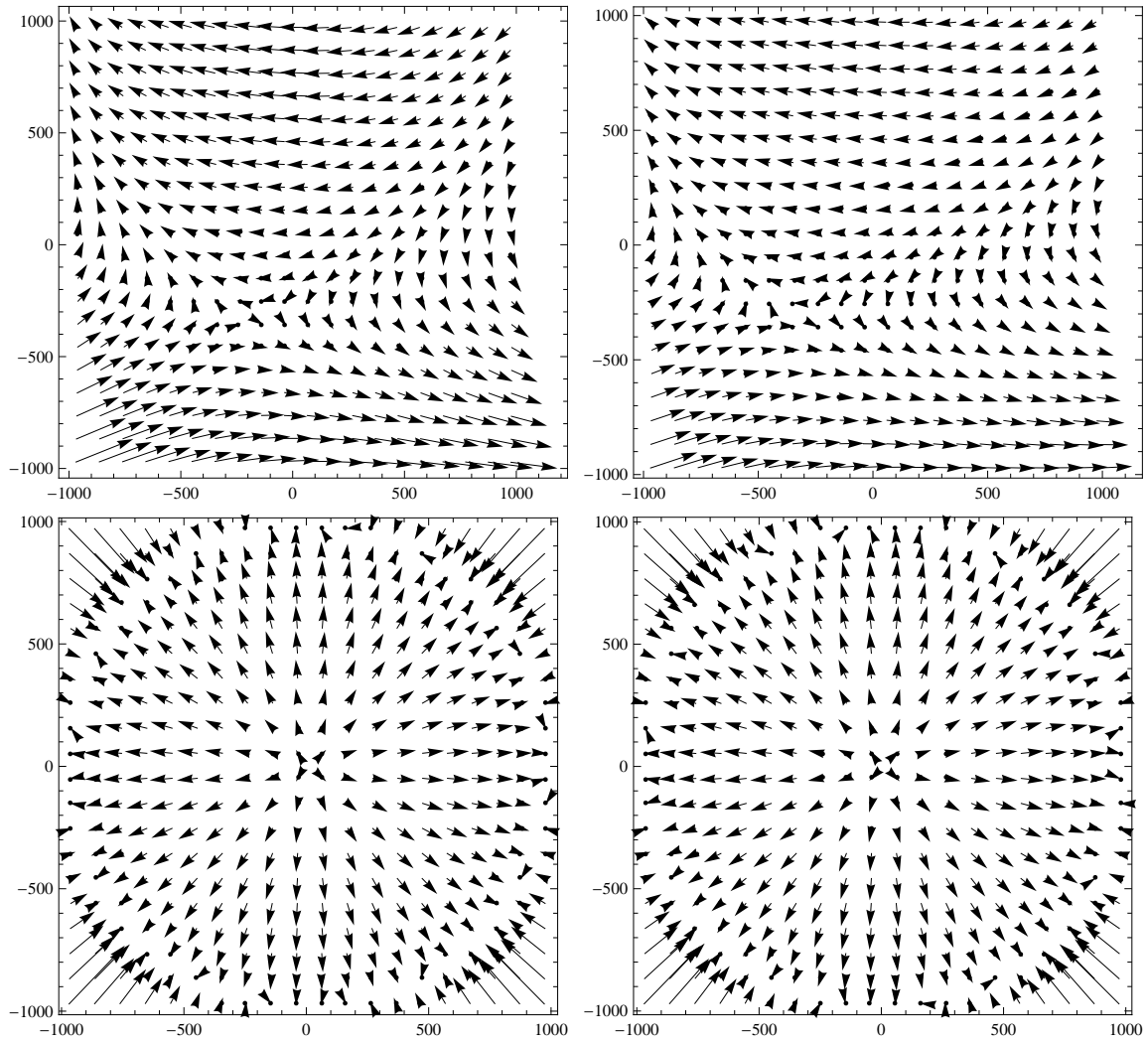


Figure 12: Residuals of the fits in Table 7 for the High-res channel for detector 0 (left) and 1 (right). Top: linear fit (residuals magnified by 10). Bottom: fit with linear, skew, and quadratic terms (residuals magnified by 100). The scale is pixels. The points are on a 100x100 pixel grid. For the residuals of all four detectors, flip the residuals of detector 0 and 1 along the top edge.

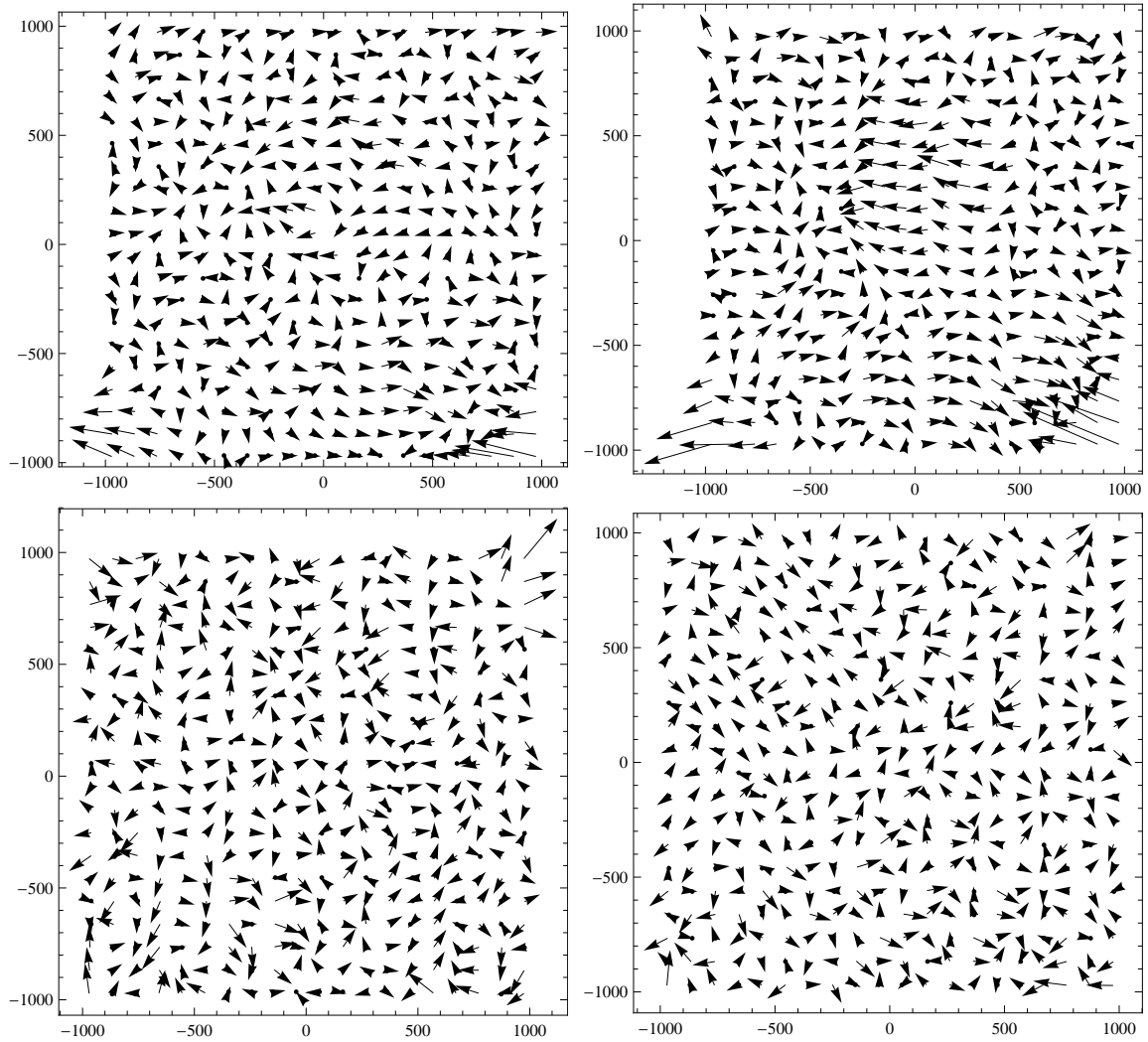


Figure 13: Residuals of the fits in Table 7 for the wide-field channel (top) and the high-res channel (bottom) for detector 0 (left) and 1 (right). The fit includes linear, skew, and quadratic, and distortion terms. The residuals are magnified by 3000.

<i>Fit</i>	<i>x-basis</i>	<i>y-basis</i>	σ_x	σ_y	max_x	max_y
<i>Wide field</i>						
linear	(1, x)	(1, y)	10	2.7	23.9	7.4
skew	y	x	2.2	0.68	8.2	3.1
quad	(x^2, xy, y^2)		0.61	0.59	2.4	2.2
distortion	$x(x^2 + y^2)$	$y(x^2 + y^2)$	0.03	0.012	0.16	0.07
cubic	x^2y	xy^2	0.023	0.02	0.12	0.06
quartic	$(x^4, x^3y, x^2y^2, xy^3, y^4)$		0.015	0.009	0.04	0.02
<i>High res</i>						
linear	(1, x)	(1, y)	7.4	2.1	21.	6.9
skew	y	x	2.5	0.82	9.2	3.8
quad	(x^2, xy, y^2)		0.63	0.63	2.3	2.4
distortion	$x(x^2 + y^2)$	$y(x^2 + y^2)$	0.017	0.015	0.05	0.05
cubic	x^2y	xy^2	0.015	0.015	0.04	0.05
quartic	$(x^4, x^3y, x^2y^2, xy^3, y^4)$		0.015	0.015	0.03	0.03

Table 7: Fits for image position for detector 1. The basis functions for a fit includes the basis functions of the preceding rows. The root-mean-square and maximum residuals are in pixels.

coef.	term	wide-field		high-res		det 2 to det 1 det 3 to det 0
		det 0	det 1	det 0	det 1	
θ_x						
a_0	1	-1149.377	1322.478	-1136.639	1302.762	+
a_1	x	1013.140	1042.578	996.208	1034.083	+
a_2	y	-19.008	-16.977	-14.982	-12.098	-
a_3	x^2	6.379	5.147	8.093	5.801	+
a_4	xy	-0.284	-0.223	0.067	0.157	-
a_5	y^2	6.732	4.989	8.015	5.895	+
a_6	$x(x^2 + y^2)$	-2.498	-2.680	-2.724	-2.750	+
θ_y						
b_0	1	-1231.443	-1223.024	-1238.165	-1250.846	-
b_1	y	1020.491	1020.755	1033.721	1035.562	+
b_2	x	2.411	4.601	-6.496	-3.274	-
b_3	x^2	0.891	0.901	1.116	1.124	+
b_4	xy	-0.316	0.052	0.394	-0.078	+
b_5	y^2	0.694	0.696	1.369	1.380	-
b_6	$y(x^2 + y^2)$	-2.560	-2.586	-2.801	-2.784	+

Table 8: Coefficients for mapping from the detector (x, y) to the sky (θ_x, θ_y) . The detector coordinates x and y run from -1 to $+1$ for each detector. The sky coordinates are in pixels of 68.47 mas for the wide-field channel and 41.38 mas for the high-res channel. The last column is the sign of the coefficients for detectors 2 and 3 relative to that of detectors 1 and 0.

3.1 Flat field

Even for uniform illumination with a perfectly uniform detector, the response is not uniform. Because of distortion of the optics, the solid angle in the sky seen by a pixel varies. The brightness in the sky $B_s(\theta_x, \theta_y)$ (photon/s/m²/sr) and the brightness on the detector $B_d(x, y)$ (photon/s/m²/pixel) are related by

$$B_d(x, y) = B_s(\theta_x, \theta_y)\epsilon(x, y)J(x, y), \quad (9)$$

where $\epsilon(x, y)$ is the efficiency and

$$J(x, y) = \begin{vmatrix} \frac{\partial\theta_x}{\partial x} & \frac{\partial\theta_y}{\partial y} \\ \frac{\partial\theta_x}{\partial y} & \frac{\partial\theta_y}{\partial x} \end{vmatrix}$$

is the Jacobian. The series expansion of the Jacobian is in Table 9. See Figure 14 for a plot of the Jacobian.

A flat-field is often used to correct for the spatial variations in the efficiency. If $B_s(\theta_x, \theta_y)$ is a constant c , then the flat-field F

$$F(x, y) = c\epsilon(x, y)J(x, y). \quad (10)$$

There is a distortion-induced nonuniformity in a flat-field. For an ideal flat field, where the illumination and detector response are perfectly uniform, the response $F(x, y) = cJ(x, y)$ is *not* uniform (Figure 15). The distortion-induced nonuniformity is, within a constant, the Jacobian. The most striking feature is caused by the distortion of the flat-fielding lens in front of each detector. The off-axis optics of the instrument make detectors 0 and 1 different. For the wide-field channel, the brightest points, near the centers of detectors 1 and 2, are 1.7% brighter than the mean, and the darkest corners, which are in detector 0 and 3, is fainter by 4.4%. For the high-res channel, the brightest points, near the centers of detectors 1 and 2, are 2.4% brighter than the mean, and the darkest corners, which are in detector 0 and 3, is fainter by 5.3%.

The true intensity I of a star

$$I = \int B_s(\theta_x, \theta_y) d\theta_x d\theta_y = \int B_d(x, y) / \epsilon(x, y) dx dy. \quad (11)$$

can be found using the flat field.

$$I = c \sum_{i,j} P_{i,j} F_{i,j}^{-1} J_{i,j}, \quad (12)$$

where $P_{i,j}$ is the image of the star and $F_{i,j}$ is the image of a flat field, both of which are made discrete by the pixels. Determining the overall scale c requires a calibrating star. The factor $J_{i,j} \equiv J(x_i, y_j)$ affects the intensity by a few percent.

term	wide-field		high-res		det 2 to det 1 det 3 to det 0
	det 0	det 1	det 0	det1	
1	0.9860	1.0150	0.9820	1.0212	+
x	0.0121	0.0101	0.0164	0.0114	+
x^2	-0.0098	-0.0104	-0.0107	-0.0109	+
y	0.0010	0.0011	0.0028	0.0029	-
xy	-0.0001	-0.0001	-0.0001	-0.0001	-
y^2	-0.0098	-0.0103	-0.0107	-0.0110	+

Table 9: Series expansion of the Jacobian $J(x, y)$ to convert brightness on the detector to brightness in the sky using 68.47-mas pixels for the wide-field channel and 41.38-mas pixels for the high-res channel.

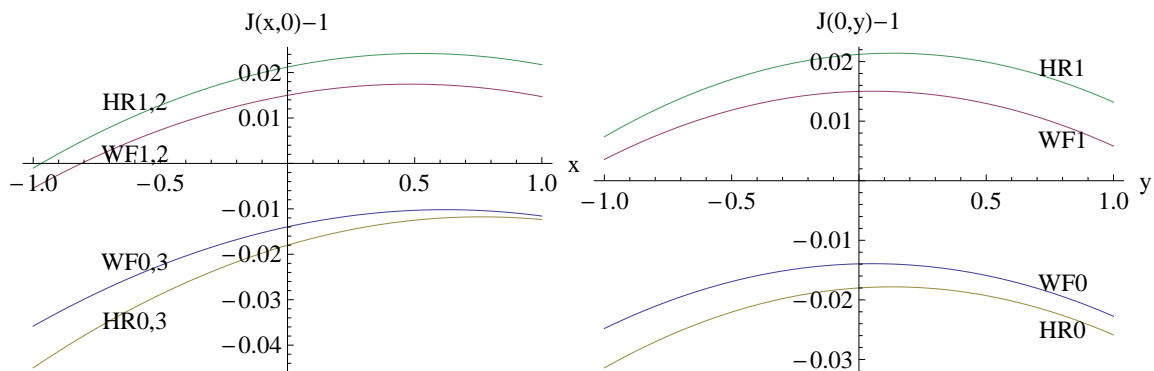


Figure 14: Deviation of the Jacobian from the nominal using 68.47-mas pixels for the wide-field channel and 41.38-mas pixels for the high-res channel for detectors 0 and 1. The y -direction is the symmetric direction. To obtain the plot in the y -direction for detectors 2 and 3, reflect the plots for detectors 1 and 0 through the vertical axis.

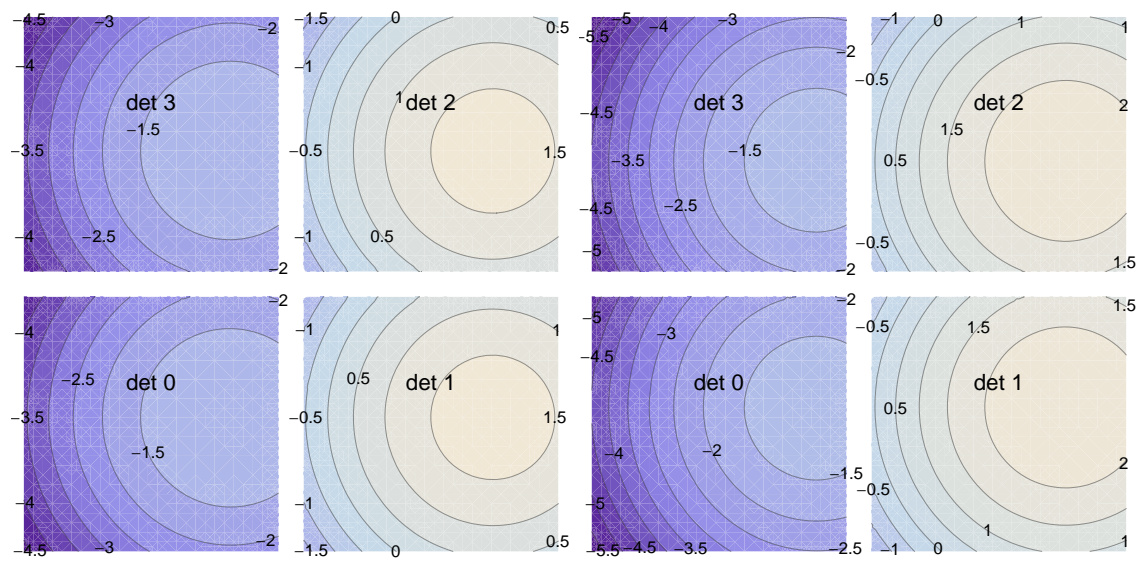


Figure 15: Ideal flat field for the wide-field (left) and high-res (right) channels. The nonuniformity is due entirely to the distortion of the optics. The contours are in percent.

3.2 World-coordinate system in the FITS header

We use the SIP convention¹¹ to represent the map between pixel coordinates (x, y) and the angle in the sky (α, δ) projected onto a plane. The coordinate type is “RA—TAN-SIP” and “DEC—TAN-SIP,” which means gnomonic projection¹² using the SIP description for distortion.

We dispense with the distinction between the angle in the sky and its projection, since the difference is negligible for our field size. With the center of projection being the center of the field, the difference between the angle and the projection is at most 0.001 pixel.

Let the map between pixel coordinates $p = (x, y)$ and the angle in the sky $s = (\alpha, \delta)$ be

$$s = M(u) + s_0,$$

where $u = p - p_0$. In the SIP formulation, $M(0) = 0$. Furthermore, M is separated into an affine transformation and a distortion function $g(u)$, a polynomial for which the lowest order term is second order. Define the affine transformation matrix C by

$$M(u) = C[u + g(u)].$$

In the FITS header, the keys CRPIX1 and CRPIX2 contain p_0 , and the keys CRVAL1 and CRVAL2 contain s_0 . The keys CD1_1, CD1_2, CD2_1, and CD2_2 contain the terms of the affine matrix C . The coefficients of g are in the keys A.i.j and B.i.j. The inverse distortion function g' , defined by

$$p = p_0 + C^{-1}(s - s_0) + g'[C^{-1}(s - s_0)],$$

is in the keys keys AP.i.j and BP.i.j. Even though the inverse distortion function is not mandatory, the program ds9 does not display the location of objects in catalogs properly without it.

The world coordinate system is derived from the measurements of stars in the sky and ray tracing of the optical design. We found a small scale error, a small rotation, and an offset.

The WCS is accurate to a few arcsec, because it is based on the accuracy of the telescope pointing. Furthermore, there is an offset that changes from picture to picture in no discernable way (Figure 16).

¹¹Shupe, D., Moshir, M., Li, J., Makovoz, D., Narron, R., & Hook, R., 2005, “The SIP Convention for Representing Distortion in FITS Image Headers,” *Astronomical Data Analysis Software and Systems XIV*, ASP Conference Series, Vol. XXX, P. L. Shopbell, M. C. Britton, and R. Ebert, eds., P3.2.18

¹²Calabretta, m., & Greisen, e., 2003, “The Representations of celestial coordinates in FITS,” *A&A*, 395, 1077–1122

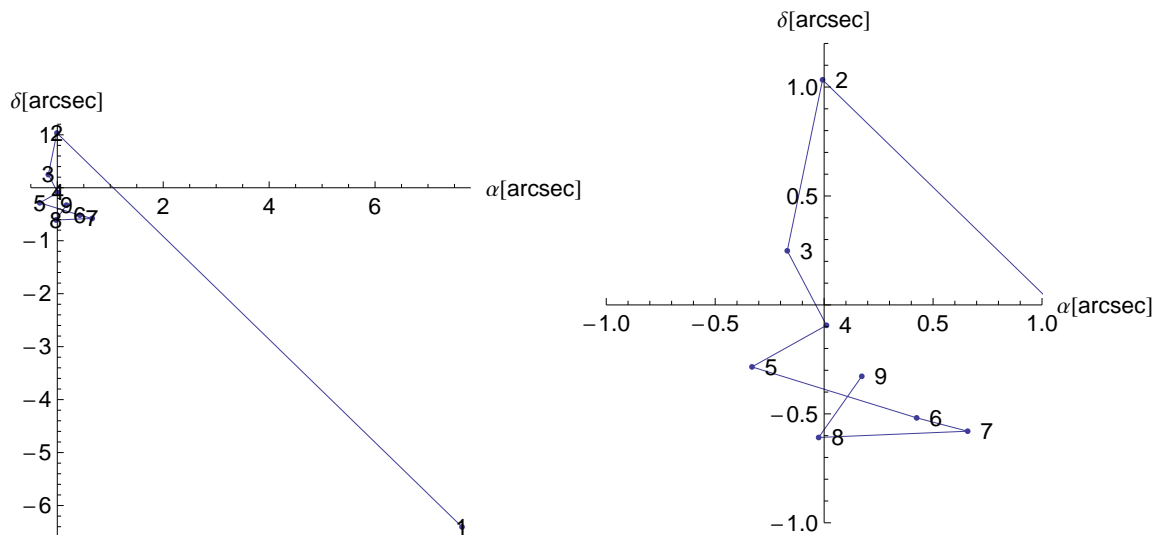


Figure 16: Location of a star derived from the WCS. The line connects successive data. The frame on the right is magnified. The telescope operator positioned the telescope for the first two images. The observer moved the telescope for images 3, 4, 8, and 9. For images 5, 6, and 7, the observer and operator did not move the telescope. The entire sequence took about 15 min.

4 Software

The software uses LabView, a graphical language, and we adopt the terminology of LabView.¹³

Much of the documentation for using the software is on the front panel of the VI. SpartanGUI has **tip strips** and **context-based help**, which explain most controls and indicators. A tip strip for a control or indicator pops up with a message when the mouse moves over it. To see the help for controls or indicators, press <cntl>+H to turn on context-based help. Then move the mouse over a control or indicator. Pressing <cntl>+H another time turns off context-based help.

There are two user interfaces, **SpartanGUI**, a graphical user interface, and **Spartan-TUI**, a rudimentary text-based user interface.

4.1 SpartanGUI

SpartanGUI is the control panel for the observer and the engineer. In normal operation, the observer need only look at this window. Status information is in the top section. The observing functions are in the observing panel. The notebook maintains a record of the observations; the observer can log comments in the notebook. To start the software, open `\homeSpartan\SpartanGUI.vi`, and the window in Figure 17 should appear. Then select the **Help** tab control for instruction. SpartanGUI has several tab controls.

Observing (Figure 17) is for the observer. The observer presses buttons on SpartanGUI to set exposure time, take pictures, change filters, and switch between the wide-field and high-res modes.

ObservingSetup (Figure 19) sets up items for the beginning of the night, the observer's name, the directory on `soaric3` in which to write images, and starting "Focusing Assistant," a Mathematica notebook for determining the best focus. Additional functions are guider information and target definitions.

Instrument (Figure 20) is to setup the detector and the mechanisms. The operations are (1) choose the detectors, (2) load the operating voltages for each detector, (3) ini-

¹³A program or subroutine is called a virtual instrument (VI). A VI has a front panel, which is for operating it, and a diagram, which is the "code." The front panel may be visible, the case for VIs that the observer controls directly, or hidden. The front panels of most VIs are kept hidden, since the observer does not need to see the internal details of the software. Controls are devices on the front panel by which the user controls the software. Examples of controls are buttons and boxes in which to enter text. Indicators are devices on the front panel by which the software gives information to the user. Examples of indicators are lights and boxes in which the software writes data.

SOAR
TELESCOPE

Spartan IR Camera

MICHIGAN STATE UNIVERSITY

ImageID: 003-9650 | ImageCopied: idle | Status: idle | PictsFree: 40

Observing | ObservingSetup | Instrument | forMechanismEngineer | InstrumentLog | MoreHelp | Help | 18:59:00

Get N Picture Pairs; N is: 1 | Remaining: 0

Target Exposure Time: 0 s | Actual: 8.5 s

Object Name: []

Filename Prefix: []

Type of Observation: Object

Change Filter to: H | 12 | See tip strip

Change Field Mask to: LRMasked | LRMasked | See tip strip

Change Pupil Stop to: LRTight | LRTight

Change Ang Res to: LowRes | LowRes

Move Focus by: 0

Put Star on: center

Offset Telescope by: [] | 61.7 | -0.5 | inst

Define as Reference: Offset from reference: 61.7 | -0.5 | inst

Move to Target: 1 | &dither 3 | 60 | 0 | inst 1

SiderealTime: 14:32:29.8 | Seeing: 0.7

ActualRADec: 14:49:24.412-30:11:56.14

RefRADec: []

OffsetRA: 0 | OffsetDec: 0

Airmass: 1 | HourAngle: -1.151

Focus: -1286 | UTC: 15:27:20.4

TeleAzElev: 090+88 | Dome: 320+00

DecPAngle: 270 | RotatorAng: -40

Inside: 12.19 degC | Out: 15.59 degC

Humidity: 30 | P: 740.9 torr

Wind: 0.2 km/h | 274 deg

Guider: x 6110 | y 9680 | err 487

Notebook | Show Contextual Help | Put Off Line | Abort | Stop

18:56:44 Defined targets: x0', x1', y1', x-1', y-1'

18:56:45 Changing/updating remote directory to None succeeded.

18:56:45 Changing observers to Nomen

Append to Notebook | Print TCS

Figure 17: SpartanGUI, the graphical interface of the software, with the observing panel selected. The menubar and run button are not shown.

tialize the mechanisms, (4) test the home positions of the mechanisms, and (5) find and store new home positions. The parameters that are unlikely to need changing are in a tab control, the two tabs of which are named Detector and PlugIn. Select the button SimulateHardware to run without any hardware. Observers should not normally use this tab.

forMechanismEngineer (Figure 21) is for monitoring the mechanisms and more detailed control of them. Normally, the mechanism moves by the amount needed to change the optic, which for example is 20° to move between filters, and this panel allows movement by steps of 0.002° . Observers should not normally use this tab.

InstLog maintains a record of mechanism movement and unexpected problems. The observer may add comments to help diagnose problems.

MoreHelp (Figure 22) contains definitions of terms, an optical schematic, and a map of the detector layout.

Help (Figure 23)

In order to reduce clutter, most of the VIs run without a visible window. To make a VI (CameraControl, LogTempPressure, MechanismInitiation, MechanismHoming, MechanismMoving, PGauge, TUI Link) visible, use the Window pulldown menu of SpartanGUI. Seeing these VIs is useful for diagnosing problems but not useful for observing.

4.2 SpartanTUI

StartanTUI is a text-based user interface for the instrument. It allows the user to run a sequence of operations using a script. To start the text-based user interface, open `\homeSpartan\SpartanTUI.vi`. The window in Figure 18 appears. Then press the run button, which is a fat arrow at the top of the window, or press `<ctrl>+R`. See §6 for detailed instructions and Table 11 for a list of commands.

The VI accepts primitive commands and scripts, for which the VI searches in “script-Folders” and if not found there, then in “defaultFolder.”

You may either run the command or script (press **Run Command**) or test it for syntax errors without running it (press **Test Command**).

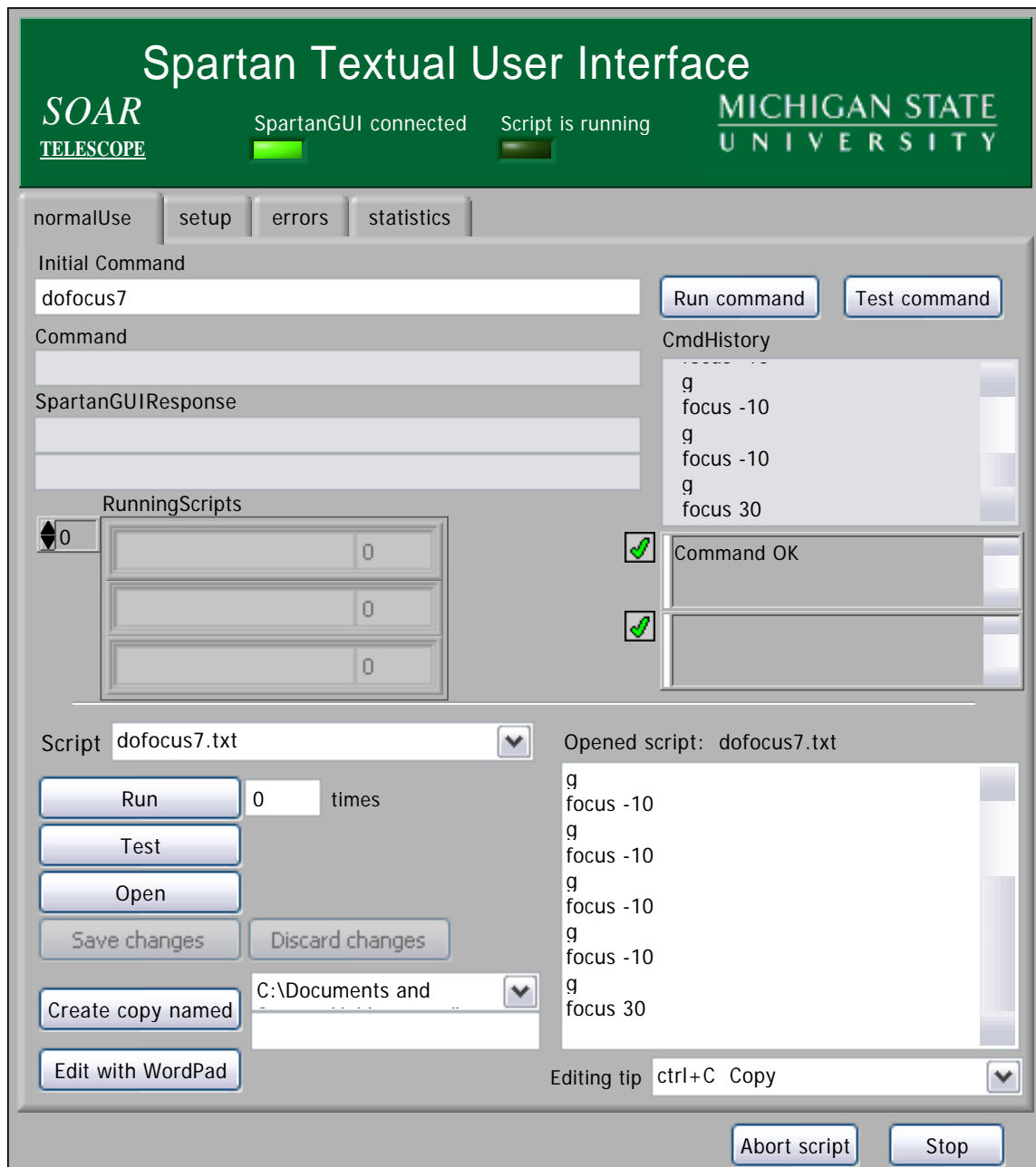


Figure 18: SpartanTUI, a text-based user interface. The menubar and run button are not shown.

4.3 Operating Other Components

Beside the user interfaces, these are the other main software components are:

Camera Control (Figure 24) controls the detector. It sends commands to the detector controller cards and receives status and images from them.

Mechanism Initialization initializes the mechanisms by initializing the motor controllers and reading the locations of each mechanism from files on the disk. The mechanisms are the filter wheel, pupil wheel, field-mask wheel, f/12 camera mirror, and f/21 camera mirror. The motor controller number and axis number on the controller are shown for each mechanism.

The status for each mechanism indicates the optic that is selected, whether the positioning is correct, and whether the position is known. The position is unknown if the computer crashed while the mechanism was being moved. The position may be incorrect if the mechanism was moved to a position between two optics; e. g. between two filter positions.

Also shown are the states of the reverse and forward limit switches. The switches are in error if both limit switches are engaged (switches are open), which is physically impossible in normal operation.

Mechanism Homing (Figure 25) locates the reverse limit of a mechanism in order to test or set its home position. Since the mechanisms do not have feedback, the position is inferred from the home position and the number of steps the motor moves.¹⁴

To save subsequent plots of the motion to find the reverse limit, which is useful for documenting problems, press the button **save plot**. The plots are saved in the directory for instrument logs, and the file name is FRL-yyyy-mm-ddThhmmss.png. For example, if the date is 1 Nov 2006, and the time is 23:15:13, then the file name is FRL-2006-11-01T231513.png.

Mechanism Moving moves the mechanisms.

¹⁴To find home, the mechanism (1) moves off of the reverse limit, if needed, (2) moves in the reverse direction until the limit switch engages, (3) moves forward slowly to disengage the limit switch, (4) moves slowly in the reverse direction to find the limit switch a second time, (5) moves to +400 steps from the reverse limit, backing into the final position to eliminate backlash. (See Figure 25 for a plot of position vs. time during homing.) Moving slowly onto the reverse limit (step 4) minimizes errors such as bouncing and delay between switch closure and sensing it. The **history** indicator shows the success or failure of each step.

To save subsequent plots of the motion, press the button **save plot**. The plots are saved in the directory for instrument logs, and the file name file name is Move-yyyy-mm-ddThhmmss.png. For example, if the date is 1 Nov 2006, and the time is 23:15:13, then the file name is Move-2006-11-01T231513.png.

Pressure Gauge reads the Inficon pressure gauge.

Log Temp Pressure maintains a log of the temperatures at several points in the instrument and the pressure inside the instrument. The **time step** is how often to save a sample in the log file. You may choose which temperatures to show on the plot. The VI records the temperature and pressure even if they are invalid.

Link to Textual User Interface implements the communication model of the observatory control system (OPEX). It receives commands from a client and passes them on to StartanGUI. In addition, it sends status to the client. The text-based user interface, SpartanTUI, is such a client.

Telescope Link queries the telescope control system for status such as the telescope coordinates and the weather.

SpartanGUIInstrumentPanel

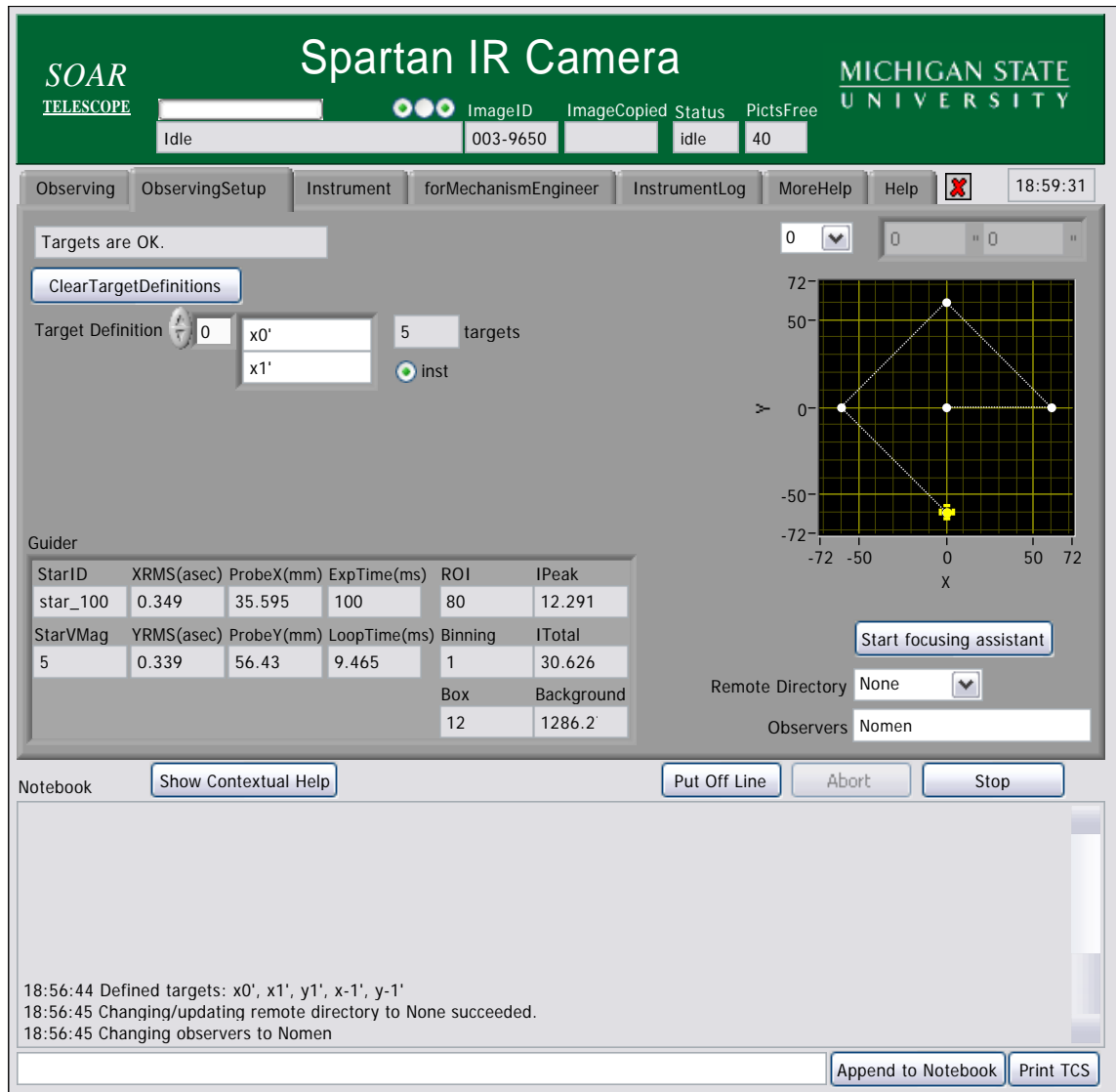


Figure 19: SpartanGUI with the panel **ObservingSetup** selected.

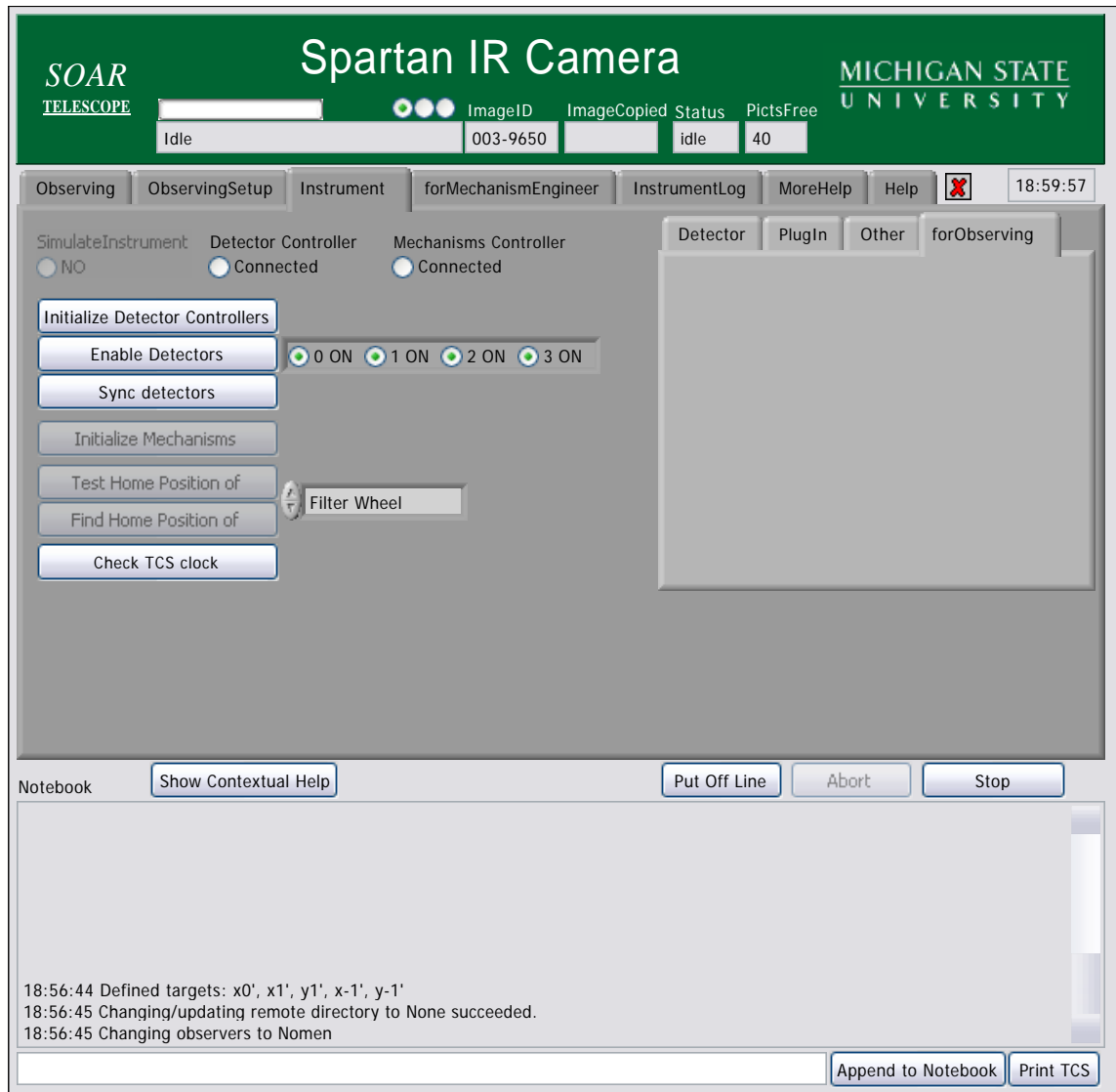


Figure 20: SpartanGUI with the panel **InstrumentPanel** selected.



Figure 21: SpartanGUI with the panel **forMechanismEngineer** selected.

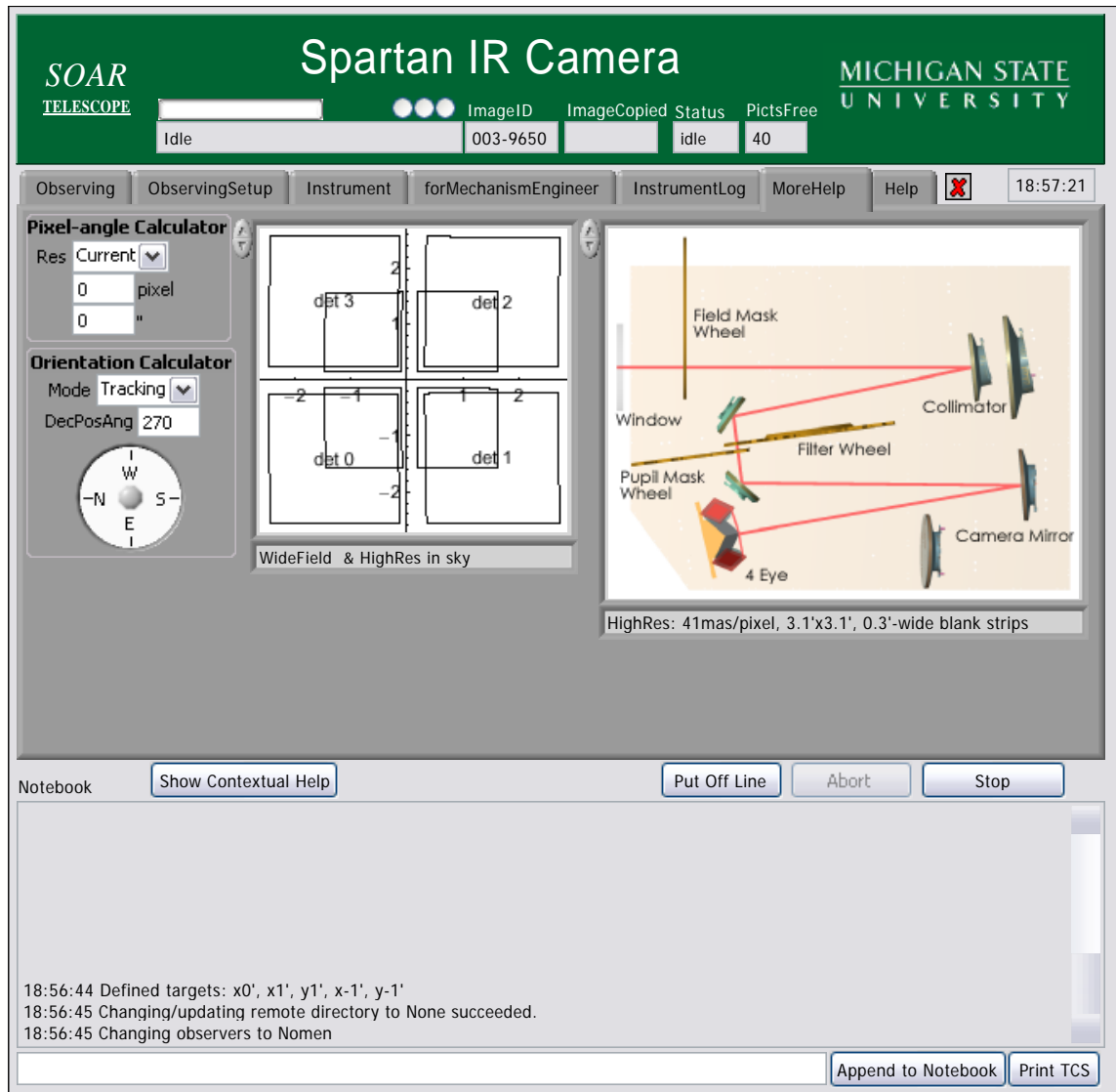


Figure 22: SpartanGUI with the panel **MoreHelp** selected.

Figure 23: SpartanGUI with the panel **Help** selected.

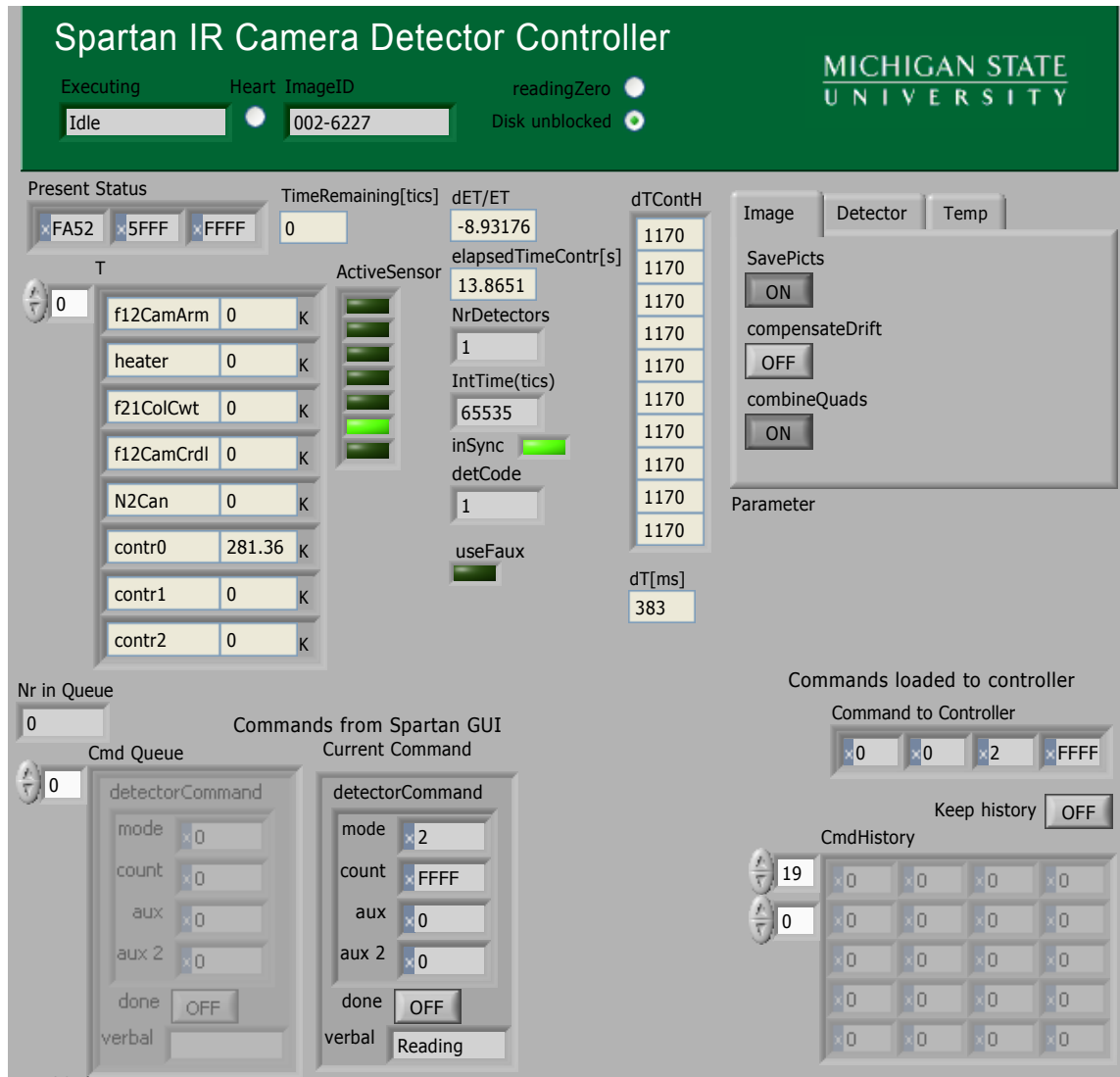


Figure 24: CameraControl, which controls the detectors. Part of the front panel is not shown.

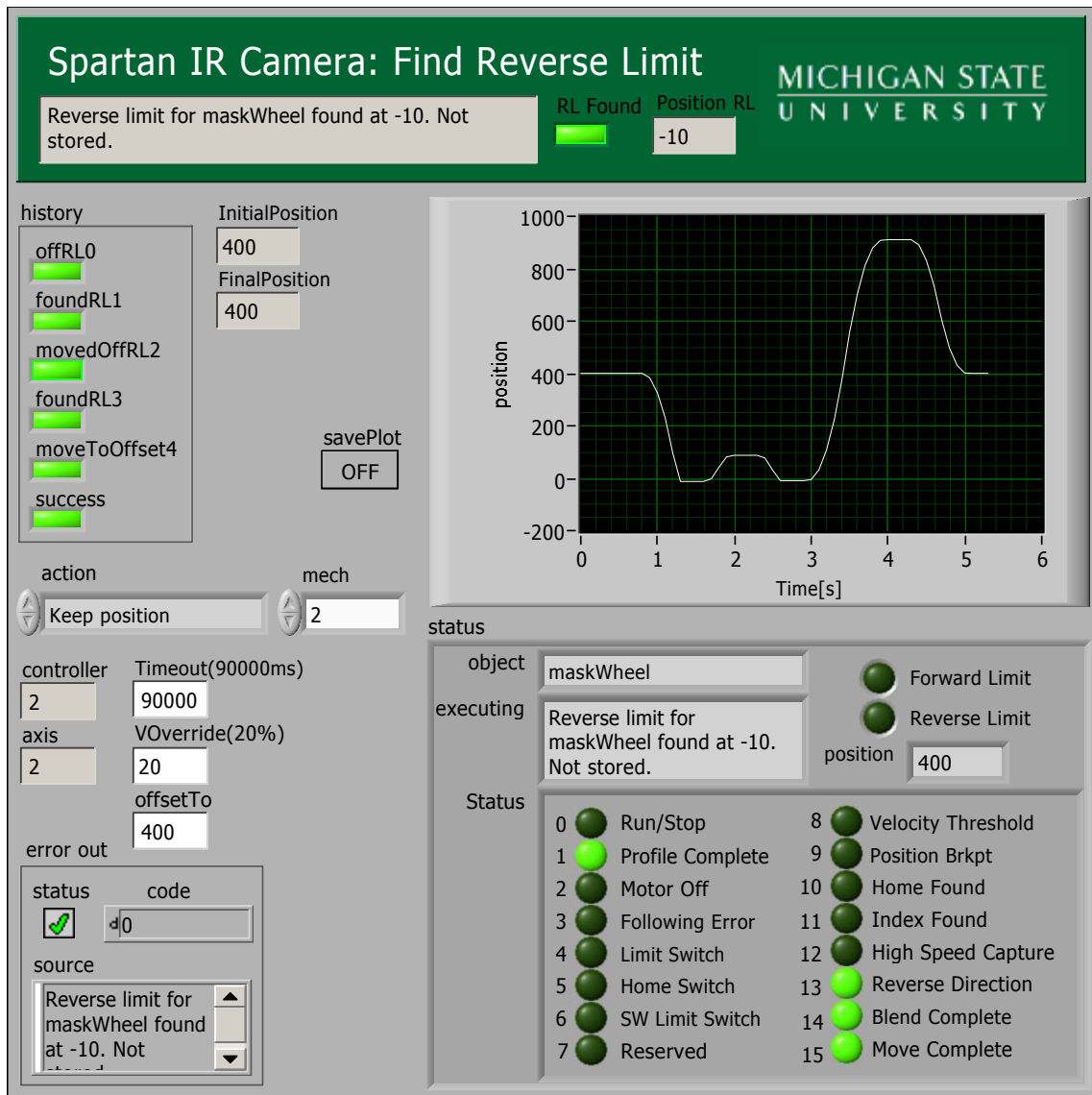


Figure 25: FindRevLimit, which searches for the reverse-limit switch of the mechanisms in order to index the position. The graph shows the position as a function of time. The mechanism moved in the reverse direction until it found the limit switch, moved forward and found the reverse limit a second time, moving more slowly, moved to 400 steps from the reverse limit, backing into the final position to eliminate backlash.

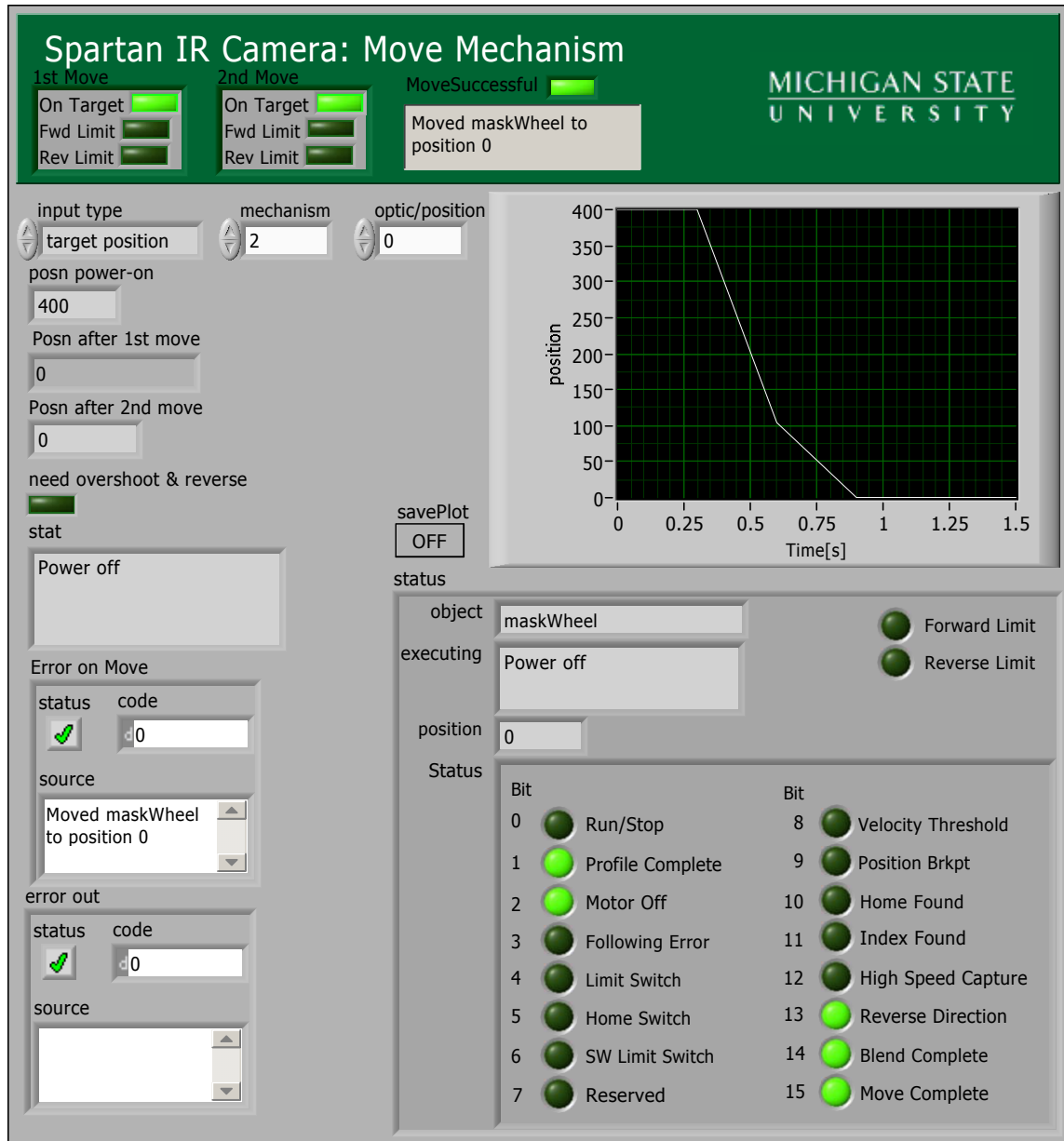


Figure 26: Move Mechanism. The graph shows the position as a function of time.

5 How to

Step-by-step instructions on common observing tasks are in this section. These instructions apply to SpartanGUI, the graphical user interface.

5.1 How to Get a Picture

To compensate for noise using a technique called “correlated double sampling,” two pictures are taken. Taking the first picture occurs immediately. Each row in that picture is read immediately after clearing the photoelectrons. This is called the “short” picture, since charge has been collecting for 0–7 ms, depending on the position of the pixel in a row. Taking the second picture of a pair, the “long” one, occurs after integrating. The second image saved on the disk is the difference between the long and short pictures. The difference is proportional to the photoelectrons collected between reading a pixel for the short image and reading it for the long image.

Clearing the stored charge is a thermal system with one degree of freedom, a capacitor (Charge is stored on capacitors, one for each pixel.) and a connection to a heat bath, the resistor. Since the time allowed for clearing the charge is much longer than the RC time, the system is in thermal equilibrium, and the noise energy is $1/2KT = 1/2Q^2/C$. The noise charge is $150 e^-$ for 1 pF and 77 K. This is called capacitor noise.

Capacitor noise is present in the short picture. After collecting photoelectrons, the long picture is read. Since the capacitor is not connected to the resistor when integrating and reading the long picture, the same capacitor noise is present in the short picture. Therefore the difference long–short is free of noise.

Select the **Observing** tab.

1. Verify the integration time, object name, filter, pupil stop, angular resolution, and filename prefix. If they are not what you want, you must change them first.
2. Set the number of picture pairs. Press the button **Get N Picture Pairs**.

5.2 How to See the Images

To see a single detector or the combined image of 4 detectors, use the button “See” in the top center of the Observing panel of SpartanGUI (Figure 17). First you must select to see either the last image or a specific image ID. You must also select either all detectors or a single detector.

5.3 How to Change the Filter

Select the **Observing** tab.

1. Select the filter and press the button **Change Filter to**.
2. If you switch between the K-band and other atmospheric bands, you may want to change the pupil stop (§5.4).

5.4 How to Choose the Pupil Stop

In the K atmospheric band, where thermal radiation of the telescope is significant, you must block the light that originates from outside the primary mirror. The “tight” pupil stops block off-mirror light for

<i>Atmospheric band</i>	<i>Low-res</i>	<i>High-res</i>
J or H	LRLoose	HRLoose
K	LRTight	HRTight

Table 10: Pupils to use with filters

all field points. Thus there is some vignetting. In the J and H atmospheric bands, the thermal radiation is insignificant. Use the “loose” pupil stops, which eliminates vignetting while relaxing the background suppression. See Table 10 for a summary of the Lyot stops.

There are several other pupil stops:

Dark slide blocks light. More precisely, it prevents light from the lit section of the instrument (left half in Figure 1) from entering the dark section (right half in the figure). The lit section includes the window and the collimators. Use this to measure the dark current of the detectors.

ND 1/10 is a small pupil that admits about 1/10th of the light for the low-res mode. Because the diameter of the pupil is smaller by a factor of 3, the diffraction width of a star is larger by a factor of 3.

ND 1/100 is a small pupil that admits about 1/100th of the light for the low-res mode. Because the diameter of the pupil is smaller by a factor of 10, the diffraction width of a star is larger by a factor of 10. Be advised that the spider on the secondary is almost in focus on the pupil stop. If the shadow of the spider happens to pass over the hole in the pupil, the amount of light is less.

5.5 How to Change Angular Resolution

Select the **Observing** tab.

1. Select the angular resolution and press **Change Ang Res**.

2. Besides moving the f/21 collimating mirror and f/12 camera mirrors to change the focal ratios, the software inserts the default field mask and pupil stops. If these are not what you want, you must change them.

5.6 How to Change Filename Prefix

The filename prefix, put at the beginning of the name of the image file, is useful for organizing your image files. Select the **Observing** tab.

1. Type in the new prefix. Keep the name brief. Spaces are converted to underscore “_.” Characters other than letters, numbers, and underscore are deleted in order that all computers can use the filename.
2. Press the button **Change Filename Prefix to**.

5.7 How to Change Object Name

The object name is stored in the FITS header. Select the **Observing** tab.

1. Type in the new object name.
2. Press the button **Change Object Name to**.

5.8 How to Focus

Focusing changes the distance between the image of the telescope and the focal plane of the instrument by moving the secondary mirror of the telescope.

A single focus applies to all filters Because the optics with any power are all reflective, the instrument is afocal. (The only exception is the field-flattening lens, which has little effect on focus.) The filters are at the pupil, where the light from a star is parallel.

Focusing should be done in the J filter, where diffraction has the least effect. On nights with good seeing, the images are indeed sharpest in the J band. On nights with poor seeing, diffraction is less of an issue, and focusing can be done using other filters.

The standard stars in the Persson catalog ¹⁵ are suitable for focusing. For example, the star Per9116, for which $J = 11.43$, $H = 11.15$, and $K_s = 11.056$, can be used with an exposure time of 30 s.

Scripts There are two sets of scripts, `dofocus__` and `dofocusstep__`, for taking the images. The scripts `dofocusstep__` move the telescope 5 arcsec between images, so that you may examine the sum of all seven images. The scripts `dofocus__` do not move the telescope. The scripts are `dofocus10`, `dofocusstep10`, `dofocus20`, `dofocusstep20`, and `dofocus50`, `dofocusstep50`. The two digits indicate the amount the secondary mirror is moved (in μm) between images. Use `dofocus10`, `dofocusstep10` if the seeing is good, `dofocus20`, `dofocusstep20` if the seeing is not poor, and `dofocus50` and `dofocusstep50` if the starting focus is very far off.

The focusing sequence must be guided, because the images are irregularly shaped without guiding.

Analyzing the images is tricky because variations in the atmosphere often change the image as much as a change in focus. Focusing Assistant, a Mathematica function, analyzes these images and provides diagnostics with which you may determine the best focus. See the following discussion.

5.9 How to Use the Focusing Assistant

The focusing assistant analyzes the set of images taken for focusing.

Starting the focusing assistant On the panel Observing Setup in SpartanGUI, press the button Start Focusing Assistant, which starts Mathematica. Skip this if Mathematica is already running. The Mathematica notebook `observing.nb` opens. Execute the command `assistant[]`, by clicking to the right of it on the notebook and then pressing `<ctrl><enter>`. (This is how all Mathematica commands are run.) Answer yes to the question of whether you want to run the initialization commands. The palette Assistants, which is a little window, should appear. I move it from the center of the screen by dragging the top bar of the palette.

What's can Assistant do? The assistant can display images by calling `ds9`, analyze a focusing sequence, and make a region to show the detector footprint on 2MASS images.

¹⁵Persson, S. E., et al., 1998, AJ, 116, 2475

To run focusing assistant You must specify the first image of the sequence and the location of the star.

1. Specify the first image of the sequence. You may either type in the name or press the button “Browse first image of sequence,” which opens a standard window for selecting a file.
2. Specify the location of the star in the first image. You may get the location using ds9 or you may type it into the palette. To find the star, use the button “See it,” which opens ds9. If you want ds9 to write the location of the star into a file, click on the star to make a region. Then save the region in the default file, ds9.reg. (Select the item “Save regions ...” on the Region menu.) Read the coordinates from the region file by pressing the button “Get star position from ds9 region.”
3. Finally, press the button “Analyze.”

The output of the focusing assistant has a summary and several panels, and the top one, called Diagnostics, is the most useful. (See Figure 27.) In the summary is the focus with the smallest image width, the focus with the lowest variance when measuring the flux of a faint star, the focus with the brightest peak, and the focus with the lowest eccentricity. If the best focus for all of these criteria agree, the best focus is likely to be reliable.

The panel called Diagnostics (Figure 27) shows plots of several quantities vs. focus. The image width is most useful. Others, which are useful for unusual images, are (1) the ratio of peak intensity to total intensity, (2) the total intensity, which should vary little, (3) the image eccentricity, (4) the orientation of the major axis of the image, (5) the variance of the flux when compared with the case of diffraction images, and (6) the image width along the major and minor axes, and full width at half maximum.

The panel named Image (Figure 28) shows each image and the residual after removing a best fit, circularly symmetric image. You may see these with an expanded intensity scale on the subpanels labeled 2, 4, and 8.

The panel called TCS shows information from the telescope control system. For the focusing sequence shown in Figure 28, the interesting item is the seeing reported by the seeing monitor. It indicates the atmosphere was changing rapidly, and therefore the focusing sequence was likely unreliable.

A focusing sequence starting with 005-5994 has better seeing, and let us find the best focus. On the panel Diagnostics (Figure 29), the plot of image width shows the width is about 400 mas for a focus of -20 , 0 , and $+10$. Therefore the image width does not define the best focus. The eccentricity is lowest at a focus of $+10$. The images residuals (Figure 30) indicate the best focus is at 0 . On the three images on the left, where the focus


```

First image          30.μm          2010-03-23T01:45:03.501 test005-8752d3
Last image          -30.           Observation title      focus
Best FWHM (on centroid) 20.   883.mas   Filter              K
Best FWHM (on peak)   20.   649.mas   Pupil stop         HRTight
Best var            30.   -5.03mag  Exposure time      20.0619
Brightest peak      20.   1924.
Lowest eccentricity -20.   0.286
    
```

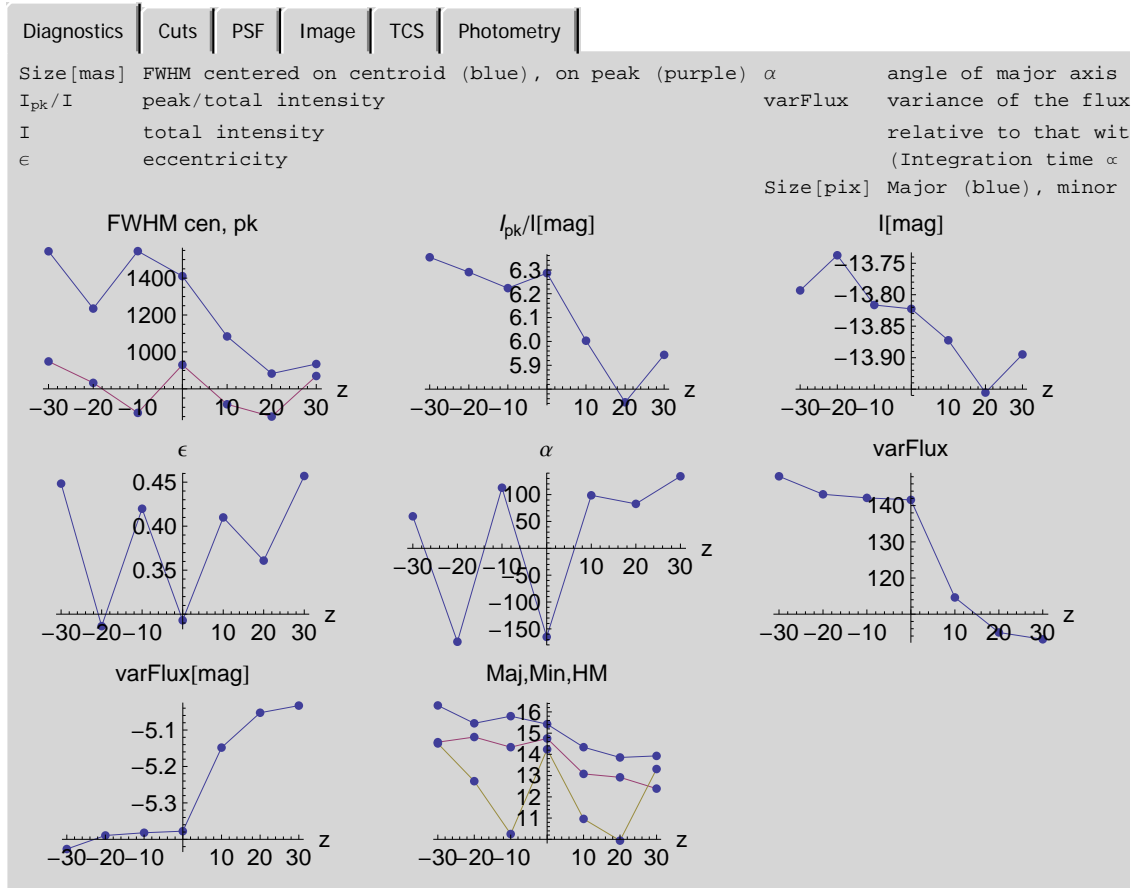


Figure 27: Focusing summary and diagnostics for the sequence starting with 005-8752

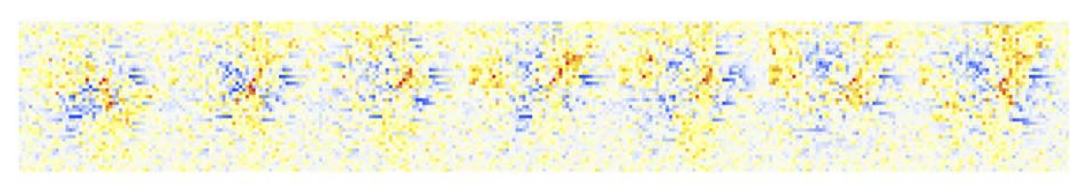
```

First image          30.µm          2010-03-23T01:45:03.501 test005-8752d3
Last image           -30.          Observation title      focus
Best FWHM (on centroid) 20. 883.mas Filter          K
Best FWHM (on peak)    20. 649.mas Pupil stop      HRTight
Best var             30. -5.03mag Exposure time    20.0619
Brightest peak        20. 1924.
Lowest eccentricity   -20. 0.286
    
```


Diagnosics
Cuts
PSF
Image
TCS
Photometry

Top: Residuals with circularly symmetric PSF (Images were taken from left to right.)
 Bottom: Images

0
2
4
8



0
2
4
8



Diagnosics
Cuts
PSF
Image
TCS
Photometry

Information from the telescope control system 08:25:28.596 -39:07:31.274
 TIME-END: 2010-03-23T01:45:23.563

SEEING	dTIME-END[s]	TELALT	TELAZ	DECPANGL	ROTATOR	TELFOCUS	AIRMASS	dRA["]	dDEC["]
1.54	0	77.7917	218.995	0.	-58.142	-1290.	1.02	0	0
1.41	40	77.7005	219.446	0.	-57.689	-1300.	1.02	0.12	0.13
1.41	79	77.6108	219.878	0.	-57.255	-1310.	1.02	-0.02	0.35
1.35	117	77.5229	220.291	0.	-56.84	-1320.	1.02	0.13	0.35
1.3	157	77.43	220.716	0.	-56.41	-1330.	1.02	-0.24	0.56
1.3	196	77.3379	221.127	0.	-55.999	-1340.	1.02	-0.24	0.75
1.3	236	77.2446	221.533	0.	-55.586	-1350.	1.03	-0.17	0.69

Figure 28: Focusing images and information from the telescope control system for the sequence starting with 005-8752

is +30, +20, and +10, the residuals are positive above and below the center. On the three images on the right, where the focus is -10, -20, and -30, the residuals are positive to the left and right of center. The images have astigmatism that changes orientation through focus, and the minimum astigmatism is at a focus of 0. The best focus is therefore at 0. The cuts across the star and the point-spread function (Figure 31) show that atmospheric variations affect the image significantly on these 10-s exposures. A longer exposure would have been better. Because of these atmospheric variations, the image width has a poorly defined minimum.

```

First image          30.μm          2009-12-02T01:38:21.545 a005-5994d3
Last image           -30.           Observation title         Per9103
Best FWHM (on centroid) 10. 381.mas Filter          K
Best FWHM (on peak)   30. 344.mas Pupil stop       LRTight
Best var             0. -3.48mag Exposure time    10.0427
Brightest peak       0. 13715.
Lowest eccentricity  10. 0.316
    
```

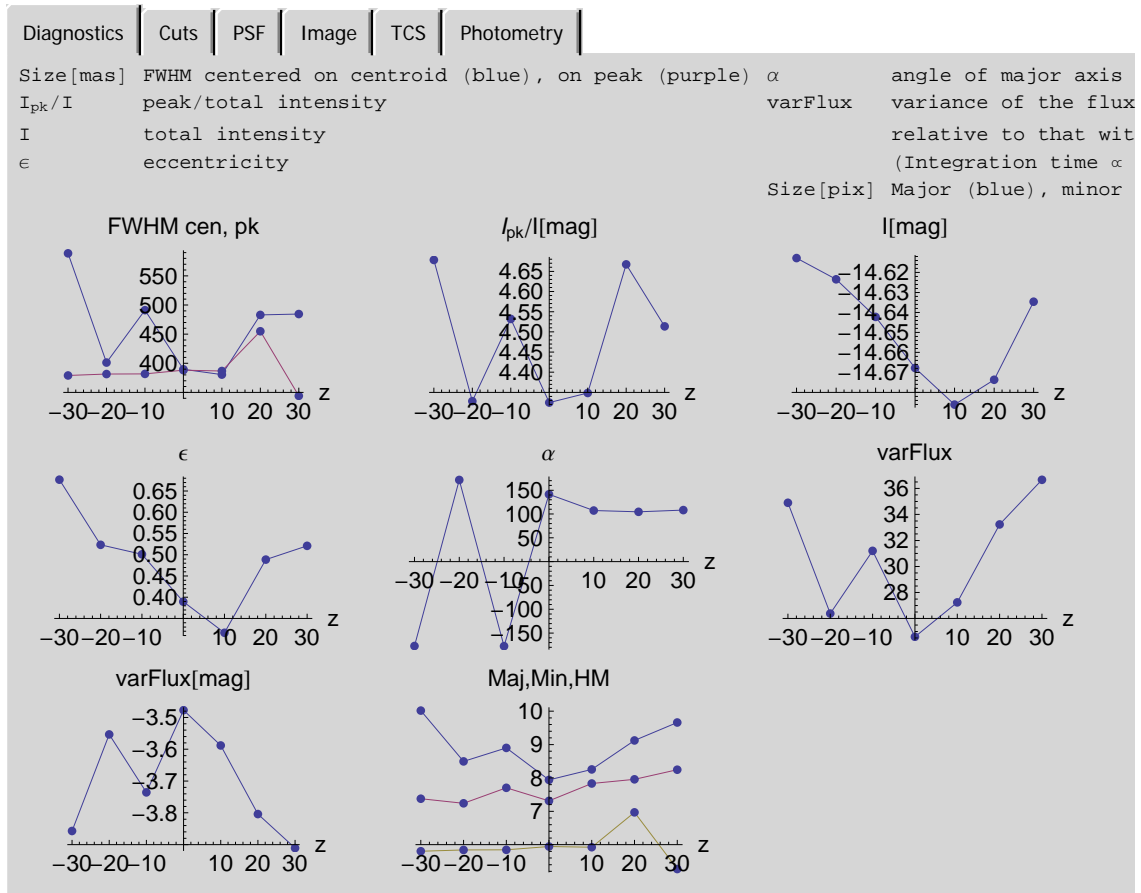


Figure 29: Summary and diagnostics for the focusing sequence starting with 005-5994, which has 380-mas seeing

```

First image          30.µm          2009-12-02T01:38:21.545 a005-5994d3
Last image          -30.           Observation title      Per9103
Best FWHM (on centroid) 10.   381.mas  Filter              K
Best FWHM (on peak)   30.   344.mas  Pupil stop          LRTight
Best var            0.    -3.48mag Exposure time        10.0427
Brightest peak       0.    13715.
Lowest eccentricity  10.    0.316
    
```

Top: Residuals with circularly symmetric PSF (Images were taken from left to right.)
 Bottom: Images

0 | 2 | 4 | 8



0 | 2 | 4 | 8



Information from the telescope control system 00:33:07.511 -39:25:40.417
 TIME-END: 2009-12-02T01:38:31.576

SEEING	dTIME-END[s]	TELALT	TELAZ	DECPANGL	ROTATOR	TELFOCUS	AIRMASS	dRA["]	dDEC["]
0.61	0	73.2924	231.888	0.	-45.643	-1152.	1.04	0	0
0.6	42	73.1712	232.123	0.	-45.427	-1162.	1.04	4.81	0.3
0.61	85	73.048	232.358	0.	-45.21	-1172.	1.05	9.55	0.44
0.61	127	72.9271	232.583	0.	-45.003	-1182.	1.05	14.52	0.63
0.63	171	72.8024	232.81	0.	-44.791	-1192.	1.05	19.77	0.77
0.63	214	72.6774	233.033	0.	-44.588	-1202.	1.05	24.79	1.09
0.55	256	72.5537	233.249	0.	-44.391	-1212.	1.05	34.57	1.08

Figure 30: Images and information from the TCS for the focusing sequence starting with 005-5994

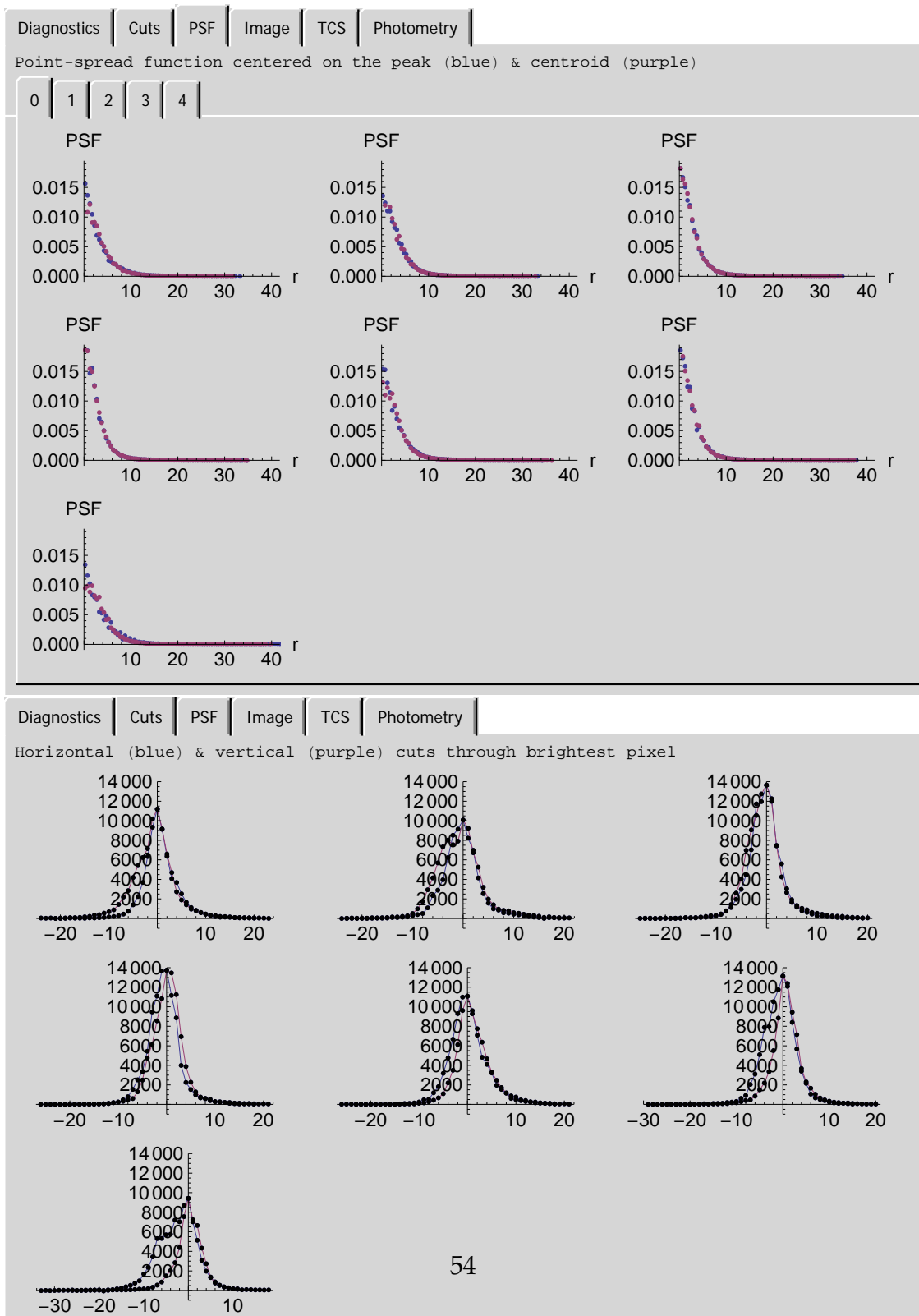


Figure 31: Point-spread functions and cuts across the images for the focusing sequence starting with 005-5994

6 Text-based Interface

For running repetitive sequences of tasks, Spartan has a text-based user interface, SpartanTUI, which passes commands to the graphical user interface, SpartanGUI.

6.1 Native Commands

Native commands (Table 11 & Table 11) are defined by the Spartan software itself. The more commonly used native commands can be abbreviated. The shortest possible abbreviations are in the tables.

Commands are not case sensitive.

Many commands require a parameter. For example, to move to a filter, the parameter is the filter name. To move to the J-band filter, type

```
filter J
```

To execute a command without a parameter more than once, type

```
<command> <number of times to execute it>
```

For example, to get 5 pictures, type

```
getpicture 5
```

6.1.1 Filters

The names used in the command `filter x` are these

<i>Loc.</i>	<i>Name</i>		<i>Loc.</i>	<i>Name</i>	
-1	K	Mauna Kea K	8	HeI/CIV	HeI/CIV 2070nm
0	H	Mauna Kea H	9	H2	H ₂ 2121nm
1	J	Mauna Kea J	10	Cont2	Continuum 2140nm
2	Y	Broad-band Y	11	BrGamma	Br γ 2161nm
3	HeI	HeI 1083nm	12	Cont3	Continuum 2210nm
4	[FeII]	[FeII] 1644nm	13	CO	CO 2325nm
5	Cont1	Continuum 2045nm	14	PupilViewingLens	Pupil viewing lens

6.1.2 Offsetting the telescope using the command `offset`

You may offset the telescope either by specifying the direction in the sky or the x and y-direction on the detector. The format for the telescope offset is direction (N, S, E, or W or X and Y), amount, and an optional unit (' (arcmin), p (pixel), or " (arcsec)), where " is the default. Examples:

```
offset N24p E3.1 ; offsets the telescope north 24 pixel & east 3.1 arcsec.
offset S5        ; offsets the telescope south 5 arcsec.
offset X23 Y3    ; offsets 23 arcsec in the x-direction & 3 arcsec in the y-direction.
```

6.1.3 Offsetting the telescope using the command `offsetTo`

You may position a star on a specific detector by means of the commands `offsetTo` and `definePosition`. For these commands, there are five positions, the center of the field, and the centers of the four detectors. The center of the field is in the interstices between the detectors, which is to the top-right of detector 0, the top-left of detector 1, the bottom-left of detector 1, and the bottom-right of detector 3.

Suppose you want a star to be centered in detector 2. After the telescope operator points the telescope at the star, the star will be at the field center. Then execute these commands:

```
definePosition c ; defines the current position as at the field center
offsetTo 2       ; puts the star on detector 2
```

Suppose you want to image a star in the other detectors after you have looked at it in detector 3. This script will do the task:

```
definePosition 3 ; defines the current position as at detector 3
offsetTo 0       ; puts the star on detector 0
g               ; gets an image
offsetTo 1       ; puts the star on detector 1
g               ; gets an image
offsetTo 2       ; puts the star on detector 2
g               ; gets an image
```

6.2 Scripts

You may write scripts, which are combinations of native commands and other scripts. To execute a script, type


```
<script name> <number of times to execute it>
```

For example, to execute the script, runHRCollimator.txt, 34 times, type

```
runHRCollimator 34
```

You may put comments in a script: What follows a semicolon “;” is a comment.

Scripts are text files <scriptName>.txt. The script name must not be the name of a native command or an abbreviation of a native command. To be safe, you may begin the name of the script with the letter “z,” which will never be used for native commands.

The software searches for scripts first in **scriptFolders** (on the front panel), in order, starting with folder 0. If not found, then the software searches in **defaultFolder**. If SpartanTUI is running as a stand-alone application, the default folder is \script in the folder of SpartanTUI.exe. If Spartan.vi is running, the default folder is \home Spartan\script.

Here are two examples of scripts. The script exerciseHRCollimator calls runHRCollimator. The script exerciseHRCollimator.txt:

```
;exerciseHRCollimator exercises the high-res collimator
; by testing home before and after 100 movements
testHome 2           ;test home position for motor 2
runHRCollimator 100 ;run script 100 times
testHome 2
```

The script runHRCollimator.txt:

```
;runHRCollimator moves the high-res collimator
; into the optical path and out
HRCollimator 0       ;move into beam
HRCollimator 45000  ;move 90 degrees
wait 60              ;wait 60s to prevent motor from overheating
```

6.3 Testing Scripts

You may test a script for syntax errors before you run it. Type the command for calling the script as you normally do, and then press the button **Test Command**, rather than the button **Run Command**.

Table 11: Commonly used text commands. The shortest possible abbreviation is underlined. Commands are not case sensitive. Some commands set a parameter. To find out the value of the parameter, type the command without a parameter. For example, `time 20` sets the exposure time to 20 s, and `time` asks for the exposure time. The query form of the command exits for commands with a “?” in the second column.

<i>Command</i>	<i>Q</i>	<i>Explanation</i>
<u>GetPicture</u>		Get picture: Read detector.
<u>Time</u> x	?	Set exposure time to x seconds.
<u>Filter</u> x	?	Move to filter x.
<u>Pupil</u> x	?	Move to pupil stop x.
<u>Mask</u> x	?	Move to field mask x.
<u>Object</u> x	?	Set object name to x.
<u>Prefix</u> x	?	Set filename prefix to x.
<u>Resolution</u> x	?	Change ang-res to x, where x is “high” or “low.”
<u>OLog</u> x		Write entry x into the observing log.
<u>ILog</u> x		Write entry x into the instrument log.
<u>Offset</u> o		Offset the telescope by o.
<u>OffsetTo</u> x		Offset the telescope to x, where x is c, 0, 1, 2, or 3, which indicate the field center, and detectors 0–3.
<u>DefinePosition</u> x		Define the current telescope position to be at x, where x is c, 0, 1, 2, or 3.
<u>Focus</u> x	?	Move the telescope focus by $x \mu\text{m}$
<u>DefineTargets</u> t	?	Define telescope targets where t is a list, separated by commas, of offsets from the reference. Example: <code>definetargets N0,N2',S2',E2',W2'</code> defines a cloverleaf pattern centered on the reference.
<u>DefineTargets</u> n t	?	Define telescope targets starting at target n, where t is a list, separated by commas, of offsets from the reference. Numbering of targets starts with zero. If n is negative or larger than the largest existing target number, the new targets are appended to the existing ones.
<u>Dither</u> x	?	Set the dithering radius to x arcsec
<u>To</u> n	?	Move the telescope to target n with dithering. Numbering of targets starts with zero.
<u>ClearTargets</u>		Clear the target definitions
<u>Reference</u>		Define current telescope position as the reference
<u>PrintTCS</u>		Print information from the telescope control system in the observing and instrument logs.

Table 12: Less commonly used text commands. The shortest possible abbreviation is underlined. Commands are not case sensitive. Some commands set a parameter. To find out the value of the parameter, type the command without a parameter. For example, `time 20` sets the exposure time to 20s, and `time` asks for the exposure time. The query form of the command exits for commands with a “?” in the second column.

<u>InitDetector</u>		Initialize detector controllers.
<u>InitMechanism</u>		Initialize mechanisms controllers.
<u>Detectors</u> n	?	Enable detectors n, where n is any combination of 0–3.
<u>Home</u> n		Move motor n to home, and reset positioning.
<u>TestHome</u> n		Test home position of motor n, but do not reset positioning.
<u>OnLine</u>		Put instrument on line.
<u>OffLine</u>		Put instrument off line.
<u>Status</u>		Query status.
<u>Sync</u>		Synchronize detector controllers.
<u>HRCollimator</u> x		Move high-res collimator to position x.
<u>LRCamera</u> x		Move low-res camera mirror to x.
<u>Wait</u> x		Wait x seconds.

7 Operating the Software with a Simulated Camera

You may operate the software with a simulated camera. For example, you can time exposures and take pictures even if the detector electronics are not installed on the computer. This is useful for learning to use the instrument.

To operate with a simulated camera, open the **Setup** panel in SpartanGUI before you run the software. Make the control **SimulateInstrument** read “Yes.” Now run the software. The banner will be “Simulated Spartan Camera,” rather than “Spartan IR Camera.”

8 Operation with a Web Browser

You may operate SpartanGUI and SpartanTUI with your web browser using “Remote Panels.” Remote Panels has two modes, viewing and control. When controlling, you can press buttons on the operator’s panel to operate the camera. When viewing, you see the operator’s panel, but you cannot control it.

To start open the URL <http://soaric3.ctio.noao.edu/SpartanGUI.htm>

To view the camera without controlling it, right click on the panel and select **Release Control of VI**.

To operate the camera, right click on the panel and select **Request Control of VI**.

You may view and control other components of the software with remote panels. The links are in Table 13.

<i>Component</i>	<i>URL</i>
Spartan GUI	http://soaric3.ctio.noao.edu/SpartanGUI.htm
Detector controller	http://soaric3.ctio.noao.edu/DetectorController.htm
Mechanism homing	http://soaric3.ctio.noao.edu/MechanismHoming.htm
Mechanism moving	http://soaric3.ctio.noao.edu/MechanismMoving.htm
Mechanism initialization	http://soaric3.ctio.noao.edu/MechanismInitialization.htm
Temperature & pressure log	http://soaric3.ctio.noao.edu/LogTempPressure.htm
Pressure gauge	http://soaric3.ctio.noao.edu/PGauge.htm
Liquid nitrogen valve	http://soaric3.ctio.noao.edu/LiquidNitrogenValve.htm
Heater controller	http://soaric3.ctio.noao.edu/Heater.htm
Image statistics	http://soaric3.ctio.noao.edu/ImageStats.htm

Table 13: Links to remote panels

8.1 Preparation

You must install LabView Run-time Engine, which includes a plug-in for the browser. For Windows NT, 2000, or XP, Download for Windows. For Mac OS X, Download for Mac. For Sun Solaris, Download for Sun. For Linux on Intel machines, Download #1 for Linux and Download #2 for Linux. Then install the software. You may use either Internet Explorer or Mozilla.

If you need to download Run-time Engine for other operating systems, go to ni.com. (1) Select Support > Driver and Updates. (2) Choose Product Line > Labview, Software > Labview Run-time Engine, Software Version > 7.1.1, and Operating System. (3) Download and then install.

These are the instructions that NI provides, but we have used them successfully only with Windows and Internet Explorer. We have had problems installing the plug-in for Mozilla on Windows and for Mozilla on a Mac.

9 Other Documentation

Spartan Documentation

- **Spartan software manual** Loh, E., 2006.
- **Spartan maintenance and installation manual** Loh, E., 2006.

10 Acknowledgement

We thank the Center for Cosmic Evolution, Michigan State University, the SOAR Telescope, the National Council for Scientific and Technological Development of Brazil (CNPq), State of São Paulo Research Foundation (FAPESP), and the National Science Foundation¹⁶ for funding this camera. We thank Jack Baldwin and Brooke Gregory for carefully reading this document and suggesting large and small ways to clarify it.

¹⁶This material is based upon work supported by the National Science Foundation under Grant No. 0242794. Any opinions, findings, and conclusions or recommendations expressed in this material are those of the author(s) and do not necessarily reflect the views of the National Science Foundation.